Determination of the mean first passage time of a vacancy in NiAl binary alloy by analytical and Adib's simulation algorithm and finding its diffusion coefficient.

by

Aman Wassie

A Dissertation Submitted to the

Department of Physics

Addis Ababa University

As a requirement for the degree of

Doctor of Philosophy in Physics

Addis Ababa University

Addis Ababa, Ethiopia

December 2012

Abstract

The mean first passage time (MFPT) and effective diffusion coefficients of a vacancy diffusing in NiAl compound via three main vacancy diffusion mechanisms are studied both numerically and analytically. These mechanisms are: the next-nearest-neighbor (NNN), the six-jump, and the triple defect mechanisms. The vacancy diffusion in the three dimensional crystal structure of NiAl is mapped onto a one-dimensional lattice sites, allowing the vacancy to hope to its nearest-neighbor with local transitions rates, $k(x_i \pm \Delta \mid x_i) = \pm\frac{D_0}{\Delta^2} e^{\mp\frac{U^{'}(x_i)\Delta}{2k_BT}}$, that is calculated from its potential profile U(x). The time evolution of the vacancy in this one dimensional lattice site is governed by a master equation in which it is evaluated numerically using *Algorithms for Brownian first passage time estimation* of Artur B. Adib where the lifetime of the vacancy in any state x_i is drawn from an exponentially distributed random number τ_i with mean equal to the reciprocal of the sum of the outgoing rates, $< \tau_i >^{-1} = \sum_{x^{'}=n.n} k(x^{'} \mid x_i)$ and the nearest neighboring site where the vacancy is going next is chosen with a probability $w(x^{'}) = \frac{k(x^{'}|x)}{\sum_{x^{'}=n.n} k(x^{'}|x_i)}$. The sum of the times $< \tau_i >$ until the vacancy touches the absorbing sites is the first passage time of that mechanism. For each mechanism, we calculate the mean first passage time of the vacancy and our result predict that the triple defect mechanism takes less time compared with the others and it is the major contributor to vacancy diffusion in NiAl binary alloy.

In the above one dimensional lattice sites, instead of the local transition rates, we allowed the vacancy to hope from any site to its nearest neighbor with local jump probability, p_i or q_i. The mean first passage times (MFPTs) for a vacancy that diffuses via the three mechanisms are evaluated using the properties of *random walks on networks technique*. These analytical result show that the MFPT of the vacancy in those mechanisms can be expressed in terms of the local jump probabilities (p_i and q_i) which in turn they are given by local MFPTs. Finally from these local MFPTs, we came up the vacancy's MFPTs to complete its mechanisms and these times are a functions of vacancy's local (E_i) as well global barrier heights (E_g), the background thermal energy (T), and the lattice space (Δ) of these mechanisms, $\tau_i \simeq \frac{4}{D_0}\left(\frac{\Delta}{\beta(E_2+E_3)}\right)^2 \exp[\beta E_g]$. Fixing the background temperature at T = 1200K and using computed local and global energies and other related parameters, we evaluate analytically MFPT of these mechanisms. This result also favored the triple defect mechanism as the main diffusion path of a vacancy in NiAl compounds, moreover, the analytical values of six-jump and triple defect mechanisms are nearly identical with the one computed by Adib's method.

The three local energy barrier heights of the six-jump and triple defect mechanisms where the vacancy crosses along its diffusion paths are summed which we call them global energy barrier heights ($U(x) = E_1 - E_2 + E_3$). From this new potential structure which is globally varying periodic potential $U(x) = U(x + \Delta g)$ with period $\Delta g = 3\Delta i$, we postulated a one dimensional random walk of the vacancy with lattice step size Δg which is the potential period and the lattice sites are centered at the global potential minima. Assuming this diffusion of the vacancy in these global

energy barrier heights as over-damped Brownian particle in a symmetric global periodic potential, we calculated the effective diffusion coefficient(D) of the vacancy in these mechanisms. Our result indicates that the effective diffusion coefficient of these mechanisms are reduced to the mean first passage time as well as the global lattice space, $D = \frac{\Delta_g}{2\tau}$. Since this, τ, is described by the local as well as global energy barrier, lattice space and temperature, therefore, taking the background temperature at T=1200K and values of computed local and global energy barrier heights and experimental values of the free diffusion coefficients (D_0) of those mechanisms, we evaluate the effective diffusion coefficient of each mechanism and we have found that the value of triple defect is 10^7 and 10^3 greater than the NNN and the six-jump mechanisms respectively. Moreover, the temperature dependence of the effective diffusions coefficients (D) of a vacancy in NiAl by these mechanisms was found to obey the Arrhenius law in the temperature interval from 1200 to 1500K.

Acknowledgments

First and foremost, I would like to express my sincere appreciation to my advisor, Mulugeta Bekele for having so much faith in me. His inspiration and motivating comments were always effective and crucial in my academic life. He allowed me to have such a freedom to do whatever I wanted to, and has been very patient.

I cannot thank Lemi Demiyu and M.s Tselat enough for their tremendous help all through the years. They helped me with administrative paper work to personal problems, and their help was always superb. Thanks all of you for your help. Last but not the least, I deeply thank all my family. My wife, Muna, understands my absence and has the endless patience. Without her love, support and encouragement, I could not finish. My little two angels, Musab and Ferha, are the main energy for me to endure the tough days and enjoy the good one. My brothers, sisters and their family, Hagose, Nega, Shifaw Bewket, Salih and all others, has been very supportive all through my life.

A special thank to Tatek Yirgu for his constructive and practical comments on coding my algorithm, and analyze my output data. I should also mention that my graduate studies in Addis Ababa University were supported by the University of Gondar.

Finally, all praise and thanks are due to Allah, without whose help and guidance

nothing can be accomplished.

Aman Wassie

Declaration

I, the undersigned, declare that this PhD dissertation is my original work and has not been submitted as a degree in any other university, and that all sources of material used for the dissertation have been duly acknowledged.

Author: Aman Wassie

This PhD dissertation has been submitted for examination with my approval as university advisor.

Research Supervisor: Mulugeta Bekele

Place : Department of Physics, Addis Ababa University.

Date: ——————————

Contents

List of Tables

List of Figures

Chapter 1

Motivation, Scope and Outline

At stoichiometric, the crystal structure of B2-ordered NiAl compound is simply primitive cubic CsCl structure which can be described in terms of the two interpenetrating α and β sublattice where Ni atoms occupy the cube corners and the Al atom occupy the cube center. The lattice parameter of this compound is 0.2887nm. The intermetallic compound NiAl exists over a wide range of homogeneity range extending a few atomic percent on either side of the stoichiometry [12]. The departure from stoichiometry is mainly accommodated by antisite defects, i.e. Ni atoms on Al sites (labeled Ni_{Al}) in Ni-rich alloys, and Al atoms on Ni sites (labeled Al_{Ni}) or Ni vacancy in Al-rich alloys. Even at the stoichiometric composition, NiAl have a triple defect structure because three defects must exist simultaneously, two vacancies on the Ni sites and one Ni atom on a Al site [20]. This asymmetry in the nature of structural defects could lead to different diffusion mechanisms at the stoichiometry as well as at non-stoichiometry.

The elementary process of vacancy diffusion in NiAl corresponds to the exchange between a vacancy and a neighboring atom. The unit step in vacancy diffusion is an atom breaks its bonds and jumps into neighboring vacant site. So during this exchange of the vacancy with a nearest neighbor atom, there will be a local disturbance of

an alloy element ordering. The three main diffusion mechanisms which have been suggested to avoid this disorder problem are:

- Next nearest neighbor (NNN) vacancy jump mechanism [14, 22]
- The six-jump mechanism (6JM)[4, 10]
- The triple-defect mechanism [15]

In this thesis we study what average time required for a vacancy to diffuse via the three main vacancy diffusion mechanisms and what will be their effective diffusion coefficients both numerically and analytically in NiAl compound. To solve the above problems numerically, we used *Algorithms for Brownian first passage time estimation* of Artur B. Adib [1] and we use random walks on networks technique which was formulated by Goldhirsch and Gefen [8] to evaluate them analytically.

This thesis is organized as follows. The three main vacancy diffusion mechanisms in B2 ordered binary alloy of NiAl are discussed in section 1.1. In chapter two we developed a one dimensional vacancy motion model in a discrete lattice sites that represent the process of vacancy diffusion in crystal structure of NiAl. This one dimensional stochastic process of vacancy diffusion is described with a master equation [9] followed by a its simulation using of Artur B. Adib [1] to calculate the mean first passage time taken by the vacancy to complete these three mechanisms. In chapter three we calculate analytically both the mean first passage time and the effective diffusion coefficient of the vacancy when it diffuse via those three vacancy diffusion mechanisms from their corresponding potential profiles using the techniques of [8]. In the last chapter we will summarize our findings and contributions and point out future directions.

1.1 Background: vacancy and its diffusion in NiAl Compounds

The intermetallic compounds with the B2 structure represent a binary ordered alloy with two sub lattices, labeled α and β, preferentially occupied by A and B atoms in a unit cell, respectively. The structure of this kind of intermetallic compound with B2-structure is shown in Fig 1.1 where α sites are at the corners and β sites at the centers of the cubic lattice cells, each β site being coordinated to eight α site. These compounds have the stoichiometry AB, where one atom type (B) is at

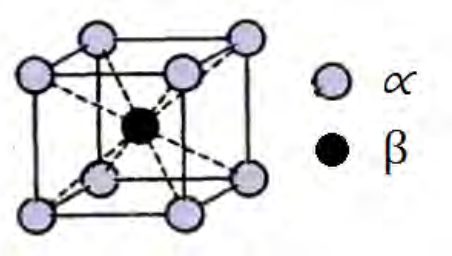

Figure 1.1: B2-ordered intermetallic crystal structure.

the center of the unit cell and the other is at the eight corners (A). For most of the intermetallic compounds with B2-structure, deviation from the stoichiometric composition is accommodated by antisite atoms Where A atoms wrongly placed on β sublattice sites and vacancies on α sites [16].

Intermetallic compounds with a B2 structure form a large group, and some representatives of these compounds are FeAl, CoAl, and NiAl. These intermetallic compounds demonstrate some properties which have been applied for technological application. The ordered NiAl intermetallic compound with B2 structure have attracted scientific attention for more than three decades because of its good mechanical properties, low density, high melting temperature and high oxidation resistance. These High melting point intermetallic compounds, specifically the NiAl has a potential for high

temperature application. These fulfill the technological requirements for components in energy conversion systems such as stationary gas turbines of power plants, internal combustion engines, heat exchangers and jet engines operating at high temperatures and in severe corrosive environments. Higher efficiencies will lead to a significant reduction in fuel consumption and a considerable decrease in exhaust gas emissions. High temperature resistant alloys based on the intermetallic compound NiAl alloyed with the refractory metals chromium, molybdenum or rhenium may fulfill the requirements as materials for prospective energy conversion technology operating up to 1300C in corrosive environments.

At stoichiometric composition, NiAl should exist in a perfectly ordered state where the Ni atoms occupy the cube corners and the Al atoms occupy the cube centers of a generalized body-centered cubic lattice. This compound has unusual mechanism of nonstoichiometry. Namely, the excess of Ni atoms in Ni-rich compositions is characterized by anti site point defects, whereas the excess of Al atoms in Al-rich compositions is accommodated through the formation of structural vacancies on the Ni sublattice [21]. In general four types of structural point defects can occur in NiAl:

1. Ni vacancies (V_{Ni}),
2. Al vacancies (V_{Al}),
3. Ni antisite atoms (Ni_{Al}),
4. and Al antisite atoms (Al_{Ni}).

Ni vacancies are atom sites normally occupied by Ni atoms in the perfect crystal from which Ni atoms are missed, the same is true for Al vacancies. A Ni antisite atom consists of a Ni atom on the Al sublattice and vice versa for an Al antisite

defect. Experimentally, Ni vacancies and Ni antisite atoms are observed to be the dominant constitutional defects in Al-rich and Ni-rich NiAl, respectively [13]. In the next sections, we are going to see details of the above three vacancy diffusion mechanisms.

1.1.1 Next nearest neighbor(NNN) vacancy jump mechanism

The next nearest neighbor jump mechanism implies that the vacancy jump in its own sublattice in a second neighbor site which is shown in Fig 1.2(a). In this figure a Ni vacancy jump along a [100] vector type. During this jump the vacancy has to make a single jump of length of lattice size over a potential energy that is shown in Fig. 1.2(b), calculated by Marino and Carter [11]. Recently, Z. Getahun, M. Asfaw and M. Bekele [22] have calculated the mean first passage times of the NNN and six-jump mechanisms. Their result indicates that at low temperature, the six-jump cycle takes shorter time while at high temperature the NNN takes shorter time than that of the six-jump cycle.

1.1.2 The six-jump mechanisms

The last two mechanisms in general refer to some cyclic mechanism, where the vacancy perform a series of nearest neighbor jumps following a definite path. The second mechanism is known with the name 6-jump cycle, first suggested by Huntington and then further analyzed by Elcock and McCombie [4]. Since this cyclic mechanism was first proposed in 1958 [4], it has been widely accepted as a main diffusion mechanism in ordered alloys. It was believed that this mechanism includes six successive cyclic displacements of a vacancy between the two sublattices [4, 10, 22]. The six-jump cycle

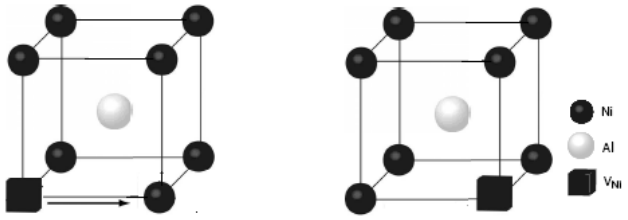

(a)

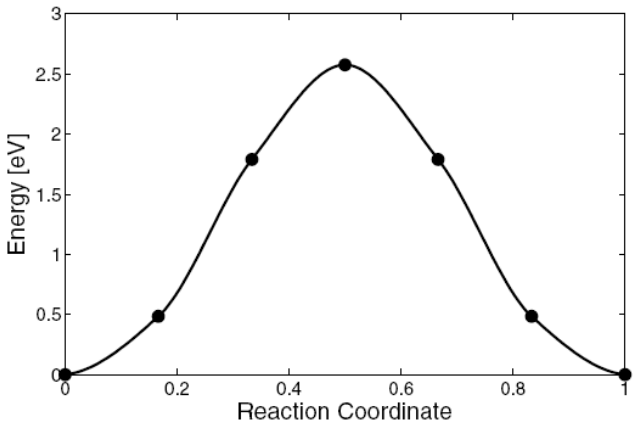

(b)

Figure 1.2: (a) A Ni vacancy due to a missing atom of Ni and its NNN diffusion path and (b) the potential profile which is calculated by [11].

in principle can occur by three different pathways, one of which results in a vacancy moving in the [110] direction whereas the other two paths move a vacancy in the [100] direction. After the six jumps, the order in the crystal is restored and the vacancy has migrated as a result of the cycle. For the first time Arita, Koiwa, and Ishioka [10], have proposed an ideal potential profile where the vacancy come across during the 6-jump cycle, which look like the following Fig. 1.3. It represents the energy change that occurs when the vacancy jumps from one state to the next state till it completes its

cycles. The following figures illustrates a 6-jump cycle occurring in a different plane

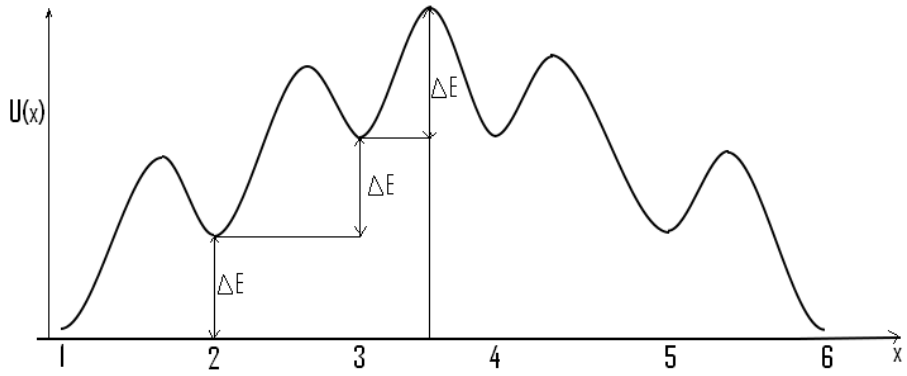

Figure 1.3: A picture which represent the energy changes of the system during the successive six-jump mechanism of a vacancy.

of NiAl compound. The first one is a cycle which is entirely contained in a [110]-type plane and the vacancy migrates by a [110]-type vector which is shown in Fig. 1.4. In the second type, the vacancy migrates by a [100]-type vector and the entire cycle

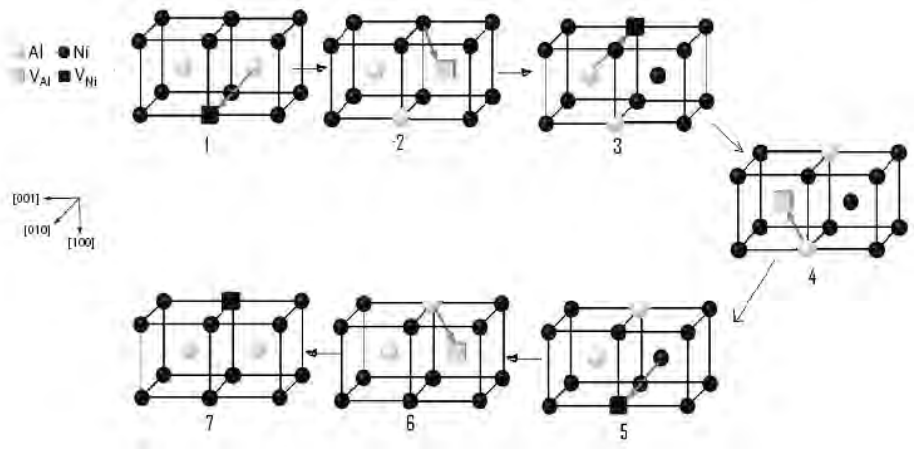

Figure 1.4: Vacancy diffusion pathway of the [110] successive six-jump mechanism.

is still contained in [110]-type plane and it is called the straight [100] cycle Fig. 1.5. The last type is a cycle in which the vacancy migrates by a [100]-type vector and the

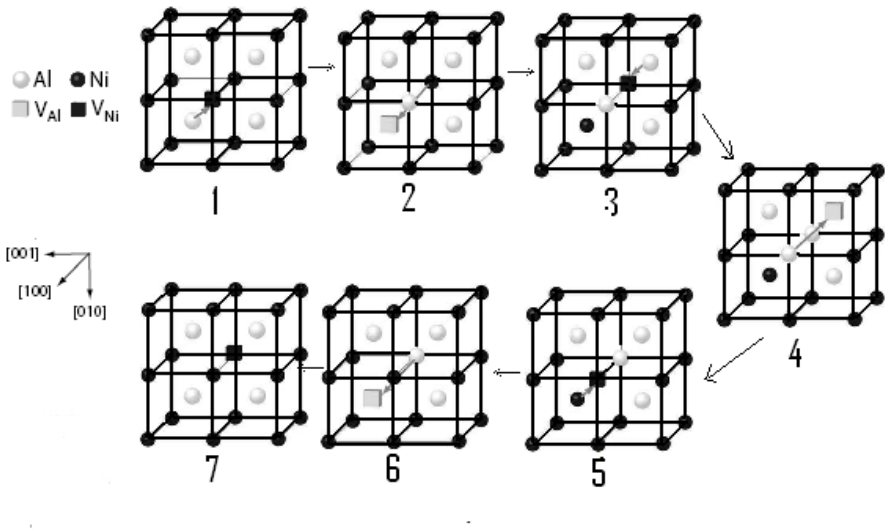

Figure 1.5: Vacancy diffusion pathway of the [100]straight successive six-jump mechanism.

cycle is not contained in a single [110]-type plane and we call it a bent [100] cycle Fig. 1.6. Recent molecular static calculations however, show that the distribution of

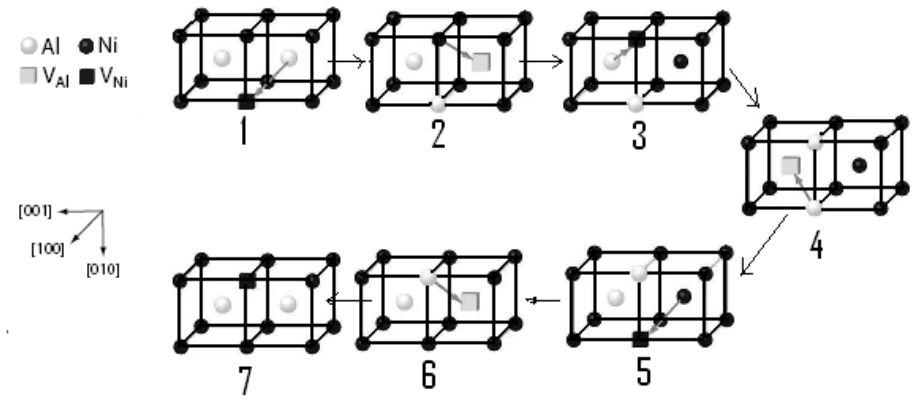

Figure 1.6: Vacancy diffusion pathway of the [100]bent successive six-jump mechanism.

energy barriers in NiAl does not follow this idealized model. Mishin, Lozovoi and Alavi [21] and Marino and Carter [11] by using first principle calculation have shown

that the conventional six-jump mechanism reduced from six to three lattice sites. As shown in those previous figures, all three cycles are proposed to start with a Ni vacancy. The first step makes this vacancy to go to Al atom, forming Al vacancy and its antisite atom. The Al vacancy moves into Ni atom creating Ni vacancy, Al and Ni antisites. The Ni vacancy fills an Al atom forming two Al antisite and Al vacancy. Because of symmetry, the second half of the cycle consists of the same NN jumps but in reverse order. But it has been shown [11] using first principle density functional theory that state 2 is unstable and Al vacancies and antisites are not typically found in NiAl [13]. Therefore, the Al and Ni atoms move at the same time and finally reach state 3 from the first state showing that sate 2 does not exist. The same happen for five and six state due to symmetry indicating state 6 is unstable. Furthermore, the configuration of two Al antisites, Ni antisite and Al vacancy is a transition state not a local minimum contrary to what was proposed previously. Therefore, due to all the above factors, one of the six-jump mechanism reduced from six to three symmetric cycles as shown in figures; Fig. 1.7.

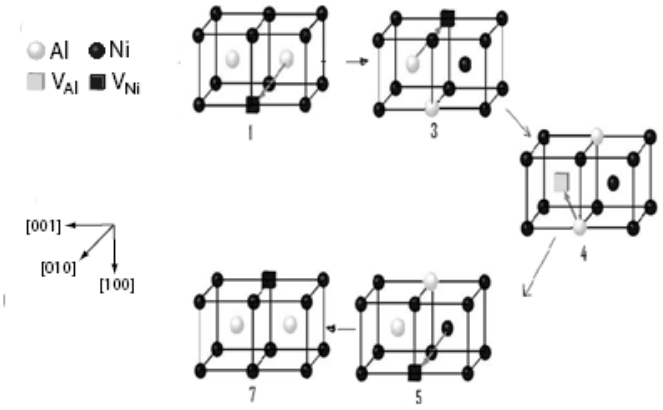

(a)

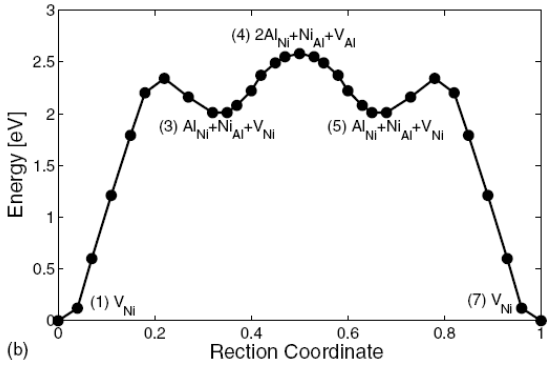

(b)

Figure 1.7: (a) Vacancy diffusion pathway of the [110] six-jump mechanism and (b) the corresponding energy profile [11] which is completed in three steps; (1) $V_{Ni} \rightarrow Al_{Ni} + Ni_{Al} + V_{Ni}$, (2) $Al_{Ni} + Ni_{Al} + V_{Ni} \rightarrow Al_{Ni} + Ni_{Al} + V_{Ni}$, and 3. $Al_{Ni} + Ni_{Al} + V_{Ni} \rightarrow \dot{V}_{Ni}$

The same is true for the remanning mechanisms that is shown Fig. 1.8 and 1.9 where the the potential profiles are calculated by [11].

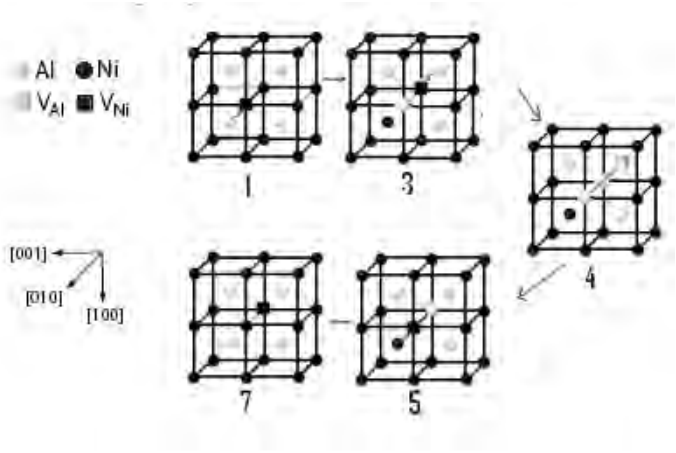

(a)

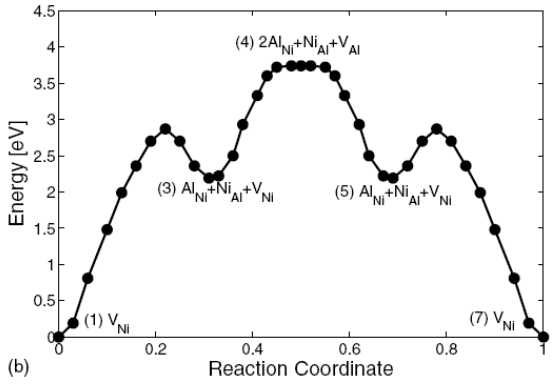

(b)

Figure 1.8: (a) Vacancy diffusion pathway of the [100]straight six-jump mechanism and (b) the corresponding energy profile [11] which is completed in three steps;1. $V_{Ni} \rightarrow Al_{Ni}+Ni_{Al}+V_{Ni}$, 2. $Al_{Ni}+Ni_{Al}+V_{Ni} \rightarrow Al_{Ni}+Ni_{Al}+V_{Ni}$, and 3. $Al_{Ni} + Ni_{Al} + V_{Ni} \rightarrow V_{Ni}$.

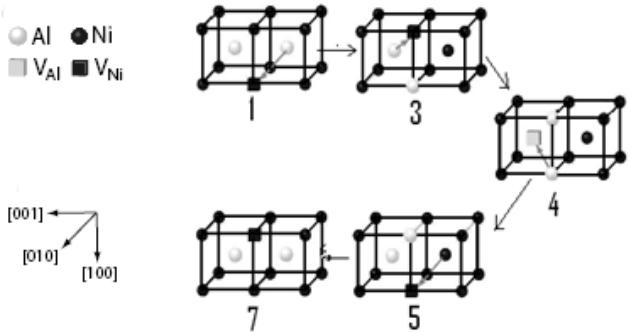

(a)

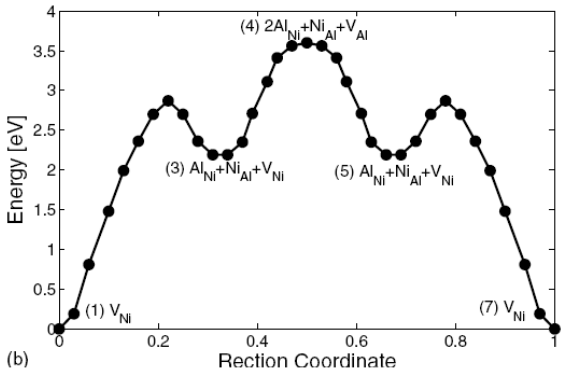

(b)

Figure 1.9: (a) Vacancy diffusion pathway of the [100]bent six-jump mechanism and (b) the corresponding energy profile [11] which is completed in three steps; 1. $V_{Ni} \rightarrow Al_{Ni} + Ni_{Al} + V_{Ni}$, 2. $Al_{Ni} + Ni_{Al} + V_{Ni} \rightarrow Al_{Ni} + Ni_{Al} + V_{Ni}$, and 3. $Al_{Ni} + Ni_{Al} + V_{Ni} \rightarrow V_{Ni}$.

1.1.3 The triple defect mechanism

The third mechanism is the triple defect mechanism where the vacancy makes some successive steps in two sublattices that is shown in Fig. 1.10(a). This mechanism was first postulated by Stolwijk [15] as a mechanism of vacancy diffusion in B2 intermetallics in their work studying diffusion in CoGa. The mechanism consists of four

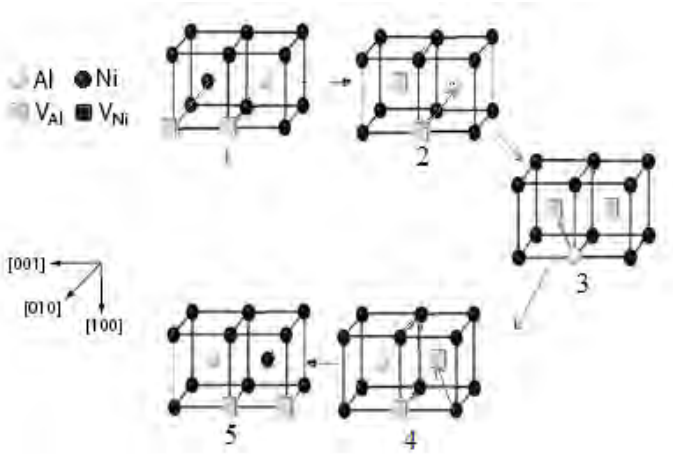

(a)

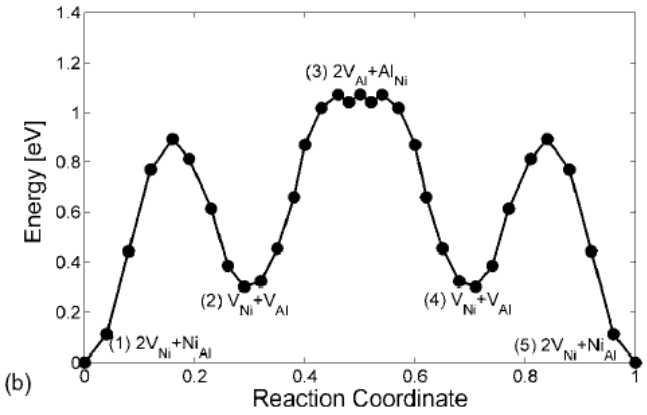

(b)

Figure 1.10: (a) Vacancies diffusion pathway of the triple defect mechanism and (b) the corresponding energy profile [11] which is completed in three steps; 1. $2V_{Ni} + Ni_{Al} \rightarrow 2V_{Ni} + V_{Al}$, 2. $2V_{Ni} + V_{Al} \rightarrow V_{Ni} + V_{Al}$, and 3. $V_{Ni} + V_{Al} \rightarrow 2V_{Ni} + Ni_{Al}$.

NN jumps initiated by a triple defect cluster comprised in the case of NiAl of two Ni vacancies and a Ni antisite atom. The first step moves one of the Ni vacancy to a Ni antisite atom, creating an Al vacancy and a Ni vacancy. Next the remaining Ni

vacancy moves into an Al atom leaving a defect cluster of two Al vacancies and an Al antisite atom. According to [11], this state is a transition state not a local minimum. From this state, One of the Al vacancy moves onto the Al sublattice and recreate a Ni vacancy and an Al vacancy. Finally the second Al vacancy moves onto the Al sublattice, leaving the final configuration of a translated Ni triple defect. Through this mechanism, two Ni vacancies shift in the same direction by a lattice vector and one Al atom moves by a lattice vector in the opposite direction. In triple defect mechanism, the vacancy completes its cycle within four lattice sites with the corresponding potential profile shown in Fig. 1.10(b) [11].

1.1.4 The Diffusion coefficient

Temperature has a most profound influence on the diffusivity and diffusion rates. It is known that there is a barrier to diffusion created by neighboring atoms those need to move to let the diffusing atom pass. In all diffusion mechanisms of NiAl alloys, a vacancy and either of the two antisites are involved, they describe coupled diffusion of vacancy and either of the elements of the alloys. Therefore, one can obtain the diffusion coefficient of vacancy, Ni, and Al atom. In this work, we try to calculate vacancy diffusion coefficients via each of those mentioned vacancy diffusion mechanisms. In general, the diffusion coefficient is characterized by the diffusion constant (D), which exhibits an Arrhenius temperature dependence where its temperature dependence can be expressed by the following equation

$$D = D_0 e^{\frac{-Q}{k_B T}}, \tag{1.1}$$

Where

- D - the diffusion coefficient ($\frac{length^2}{time}$)
- D_0 - the maximum diffusion coefficient
- Q - energy for diffusion
- T - absolute temperature and k_B - Boltzman‘s constant.

The diffusion coefficient is a function of crystal structure, temperature and material concentration. But the energy (Q) and the pre-exponential factor D_0 are constants for a given diffusion path. R. Drautz and M. Fahnle [3] have calculated the diffusion coefficients of a vacancy when it diffuse via an ideal six-jump as well as modified three jump cycles using rate equation and their results are very similar with the earlier work of Arita [10], where he used mean-first passage method to compare the diffusion coefficients of the Al and Ni atoms.

Chapter 2

One-dimensional vacancy motion in NiAl

2.1 Introduction

Stochastic processes [6, 9] by which we mean, in a loose sense, systems which evolve probabilistically in time, or more precisely, system in which a certain time dependent random variable $\mathbf{X}(t)$ evolve with time. One can measure values $x_1, x_2, x_3, \cdots$ of $\mathbf{X}(t)$ at times $t_1, t_2, t_3, \cdots$ with a set of joint probability densities $p(x_1, t_1; x_2, t_2; x_3, t_3; \cdots)$ that describe the system. A very classical example of a stochastic process is the Brownian motion, i.e. the Brownian particle is constantly buffeted on a very short time scale by the random collisions with fluid molecules. The stochastic variable $\mathbf{X}(t)$ in this case may be the position or velocity of the Brownian particle. If x were deterministic, we could find an expression for the evolution in time of x , such to give x at each t. But x is a stochastic variable, each t doesn't have a specific value for x, but a probability for x's value. Because of the above reason and its simplicity, the Brownian dynamics has been considered as a models that represent temporal evolution of systems displaying stochastic behavior. Fig. 2.1, shows the first passage time problems of this Brownian particle in specified region [x, 2Δ]. In this figure, there are two different trajectories that shows this first passage time problem. One

of this is a wiggly black line which characterize a trajectory that start from x = 0 at t = 0, and cross the absorbing boundary $x = 2\Delta$ only once at some time $t = \tau$; τ is thus the first passage time of the trajectory. This trajectory of Brownian particle are obtained by discretizing the Langevin equation in time. i.e,

$$x(t + \Delta t) = x(t) + \sqrt{2D\Delta t}\xi \tag{2.1}$$

Here $\Delta t = \tau$ is the time step, ξ is a Gaussian random number of zero mean and unit variance, and D is the diffusion coefficient. Choosing the discrete time step τ, one can move the particle with probability p to its right or q = 1 - p to its left until it reaches its absorbing site [2]. The second is a straight blue line trajectory which is a result of

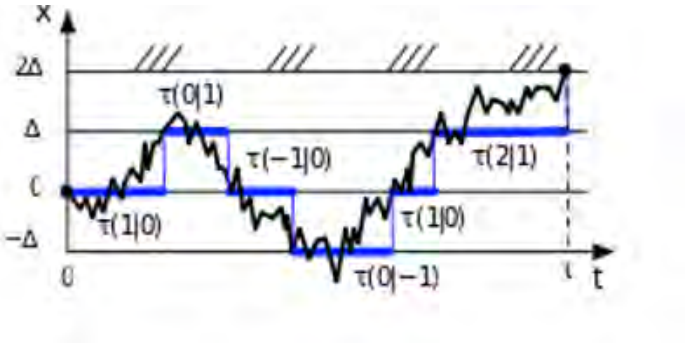

Figure 2.1: A continuous Brownian trajectory (wiggly black line) and its discrete counterpart (straight blue lines) in the first passage problem of Brownian particle [1].

the recent new first passage time algorithm of Brownian dynamics of Adib [1] where he treats space in discrete and time continuous form. It is a continuous trajectory that start from x = 0 at t = 0, and cross the absorbing boundary x = $x = 2\Delta$ only once at some time $t = \tau$. In short he took the continuum analog of Eq. 2.1 with respect

to the time by discretizing the Brownian particle path into uniformly spaced lattice in which the particle jumps with only nearest neighbor lattice sites with a transition rate k_{ij}. i.e, the transition rate from state j to state i that may depend on the location along its path. He treated the time evolution of this dynamics by rate equation [9] and then simulate this rate equation with Stochastic Simulation Algorithm (SSA) [7]. It can be seen clearly from the figure that both models demonstrate the first passage time of Brownian particle in the specified position range. In comparison the first formalism is based on the assumption that position changes are made at each time step (with a probability p of going up and 1-p of going down) at equal time intervals $\Delta t = \tau$ but the second one relaxes this restriction since it assumes that time interval between transitions are not constant but random and continues.

In this figure, one can see that the first passage time of the Brownian trajectory can be decomposed as a sum of intermediate times $\tau(x_i + 1 \mid x_i)$. Thus, the mean first passage time from state x_1 to state x_N in the restricted ensemble of trajectories that pass through a given time ordered sequence of states $x_N = (x_1, x_2, \cdots, x_N)$ is simply the time for each path times the probability of the path, averaged over all trajectories that could be given by

$$< \tau(x^N) >= \sum_{i=1}^{N-1} p_N < \tau(x_i \pm 1 \mid x_i) > \tag{2.2}$$

where the quantity $< \tau(x_i \pm 1 \mid x_i) >$ is the mean first passage time from state x_i to state $x_i \pm 1$ of a specific path to the boundary that starts at x=0.

2.2 Set-up of the vacancy diffusion model

As we have seen in the first chapter, the vacancy may take some number of jumps through the crystal structure of NiAl to complete each of those diffusion mechanisms by crossing its potential profiles like that is shown in Fig. 2.2. Then all vacancy

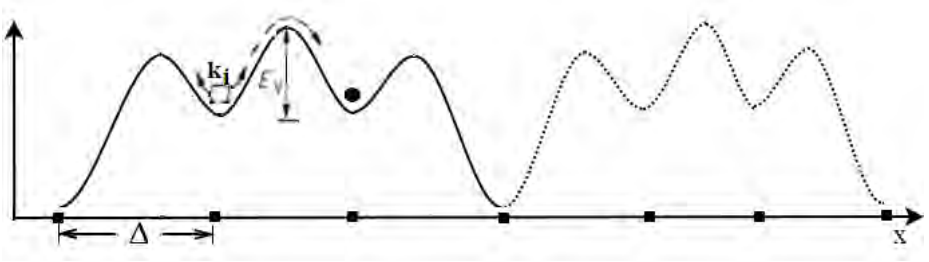

Figure 2.2: The site exchange of a vacancy with an atom by crossing an energy barrier along the one dimensional lattice .

diffusion process could be expressed in one single statement, *An atom /vacancy after having activation energy Em (thermal energy), it jumps from one site to the next* (Δ) *through site exchange with a vacancy by crossing an energy barrier with some transition rate.* Since each state to which the vacancy jumps is either stable or metastable,

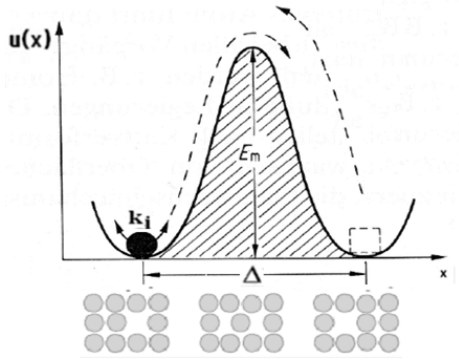

Figure 2.3: Schematic representation of the diffusion of an atom from its original position into a vacant lattice site and vice versa.

jumps of vacancies are thermally activated and each jump from one site to each neighbor sites occur with some transition rate where these rates at each state may depend on the corresponding potential profile along its path. Therefore, it is reasonable to consider each jumping process as independent of its previous one. In other words, the jumps of a vacancy between the various states represent stochastic process. In general, the different vacancy diffusion mechanisms that we have mentioned in the above are a vacancy jump from one site to the next through site exchange with an atom by crossing an energy barrier Fig. 2.3. During each vacancy jump from one site to its next one, there is uncertainty of knowing

1. what controls the rate of the vacancy/atom?
2. How do a vacancy/atom decide which way to jump and do occupy next nearest neighbor site?
3. when a vacancy jump occurs?

Which models (among the possible) could answer the above questions of motion of a vacancy in the crystal structure of NiAl both numerically and analytically?

Choice of models depend up on the type of question that we want to answer. Therefore, to answer the above questions numerically as well as analytically, we use stochastic Simulation Algorithm of Adib [1](a first passage time estimation of a Brownian particle on discrete lattice) and random walk on networks technique of Goldhirsch and Gefen [8] respectively.

The simplest approach for describing stochastic processes, which captures most of its basic essence, is to consider a random walk on a one dimensional lattice. Hence, we model the dynamics of 3-dimensional vacancy diffusion over crystal structure of

NiAl as a one dimensional nearest-neighbors hopping process, Fig. 2.4. In the figure, as we may see, it is one dimensional lattice $x_i = i\Delta$ with a lattice space Δ and $i = 0, \pm 1, \pm 2, \cdots$. In short, we consider the continuous time dynamics of a random

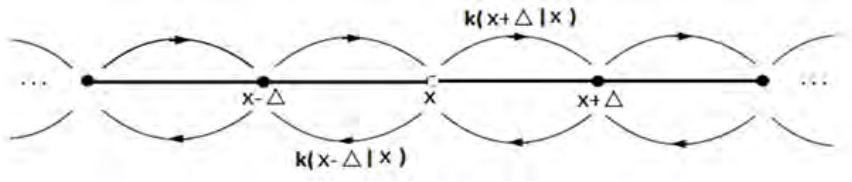

Figure 2.4: A multistate stochastic one dimensional lattice model. A vacancy in state x can make a forward transition at rate $k(x+1 \mid x)$, or it can undertake a backward transition at the rate $k(x+\Delta \mid x)$.

walk of vacancy on a discrete one dimensional lattice with nearest neighbor hopping. The vacancy jumps from site x to site $x+\Delta$ with transition probability per unit time $k(x+\Delta \mid x)$, or to site $x-\Delta$ with transition probability per unit time Δ. After moving 3 sites forward or backward the vacancy comes to the same state but shifted by a certain step size distance (3Δ). The dynamics of the vacancy can be viewed as the motion of the particle on a periodic one-dimensional lattice with a period 3Δ. To describe the stochastic behavior of our model of vacancy diffusion, let us define one more quantity $P(x,t \mid x_0,t_0)$ which denotes the probability that the vacancy is at position state being equal to x at time t given that the state was at position x_0 at time t_0. Then the time evolution of this probability distribution can be approximated by the following difference equation: for simplicity we use p(x,t) instead of $P(x,t \mid x_0,t_0)$

$$\begin{aligned} p(x,t+\Delta t) = {} & p(x+\Delta,t)k(x \mid x+\Delta)\Delta t + p(x-\Delta,t)k(x \mid x-\Delta)\Delta t \\ & + p(x,t)[1 - k(x+\Delta \mid x)\Delta t - k(x-\Delta \mid x)\Delta t] \end{aligned} \tag{2.3}$$

What does this equation mean?

Suppose at time t the state of the system, i.e., the the position of vacancy is known. What then is the probability $p(x, t + \Delta t)$ of there being a vacancy at position x at time $t + \Delta t$? where Δt is considered sufficiently small that only one transition(jump) of vacancy can occur. There are three possibilities:

1. There is vacancy coming from x-1 at time t, and jumping takes place in time Δt which gives a contribution to $p(x, t+\Delta t)$ equal to $k(x \mid x-\Delta)\Delta t p(x-\Delta, t)$.

2. There is a vacancy coming from x+1 at time t, and jumping takes place in time Δt which gives a contribution to $p(x, t+\Delta t)$ equal to $k(x \mid x+\Delta)\Delta t p(x+\Delta, t)$.

3. No jumping takes place, the probability of which is given by p(x, t) multiplied by $[1-k(x+\Delta \mid x)\Delta t - k(x-\Delta \mid x)\Delta t]$, where the latter term is given by the total probability equal to 1 minus the probability that one of the two reactions takes place.

The first two terms on the right-hand side describe jumping to position x from $x + \Delta$ and $x - \Delta$ respectively, the last term expresses the probability that during a (sufficiently small) time Δt, the jumper is at x at time t, remains at position x from t to $t + \Delta t$. By putting these three terms together and rearranging them and letting $\Delta t \to 0$, we get the master equation:

$$\begin{aligned}\frac{dp(x,t)}{dt} &= k(x \mid x+\Delta)p(x+\Delta, t) + k(x \mid x-\Delta)p(x-\Delta, t) \\ &\quad -[k(x+\Delta \mid x) + k(x-\Delta \mid x)]p(x,t) \end{aligned} \tag{2.4}$$

For n possible of nearest neighbor positions, this equation can be generalized as follows:

$$\frac{dp(x,t)}{dt} = \sum_{x'=1}^{n} [k(x \mid x')p(x';t) - k(x' \mid x)p(x;t)] \tag{2.5}$$

where

- $k(x \mid x')$ and $k(x' \mid x)$ are the forward and backward transition rates of the vacancy from site x.

This is the Master Equation (ME) which describes the time evolution of the vacancy. One of the most important useful quantities that one can determine from this equation about the vacancy diffusion process is the average time that it takes to reach a particular site for the first time. This quantity is called the first passage time and this time can be determined by imposing an absorbing boundary at state $x = 3\Delta$ in that one dimensional lattice site, Fig. 2.2.

2.3 Calculation of vacancy transition rates

The vacancy transition rates (jump probability per unit time) at each meta stable or stable state along those previously proposed diffusion mechanisms will be calculated with Adib's method [1] where he has calculated the transition rate of a Brownian particle from the local potential profile that the particle crosses. In other word, for one dimensional Brownian particle motion which is governed by the Smoluchowski equation [6] and subject to an arbitrarily shaped potential landscape U(x) (in units of k_BT), the forward and backward transition rates, $k(x \pm \Delta \mid x)$ of this particle from

any site x is given by

$$k(x \pm \Delta \mid x) = \pm \frac{D_0 U^{'}(x)}{\Delta x} \frac{1}{e^{\pm U^{'}(x)\Delta x} - 1} \tag{2.6}$$

In this equation when Δx is very small, one can write the above equation in the following form

$$k(x \pm \Delta \mid x) = \frac{D_0}{(\Delta x)^2} \left(1 \mp \frac{U^{'}(x)\Delta x}{2} + \cdots \right) \tag{2.7}$$

or in simple form

$$k(x \pm \Delta \mid x) = \frac{D_0}{(\Delta x)^2} e^{\mp \frac{U^{'}(x)\Delta x}{2}} \tag{2.8}$$

Where

- $U^{'}(x)$ is the partial derivatives of the potential evaluated at the position corresponding to the site x,
- Δx -the distance between consecutive states;
- D_0 - the free diffusion coefficient.

Using this equation, let us calculate the transition rate of the vacancy from their potential profiles at each states along each path of those vacancy diffusion mechanisms. Because we are dealing one dimension, let us take Δx as Δ from now on.

2.3.1 Six-jump mechanism

The three different six-jump vacancy diffusion mechanisms and their potential profiles are discussed in chapter one. Note that these potential profiles represent the energy changes that will occur when the vacancy jumps of lattice size $\Delta = \Delta s$ from one state to the next in NiAl crystal. Using the above techniques one can calculate the transition rates from these energy barrier heights at each lattice point. As you have seen, the three potential profiles have different local and over all energy barrier heights but three of them have nearly the same structure. Therefore, instead of dealing with each mechanism, let us take one model potential profile which represent three of them like of Fig. 2.5. In this figure, ΔE is the difference in energy between the two consecutive sites. The vacancy with the help of thermal kick should cross these energy

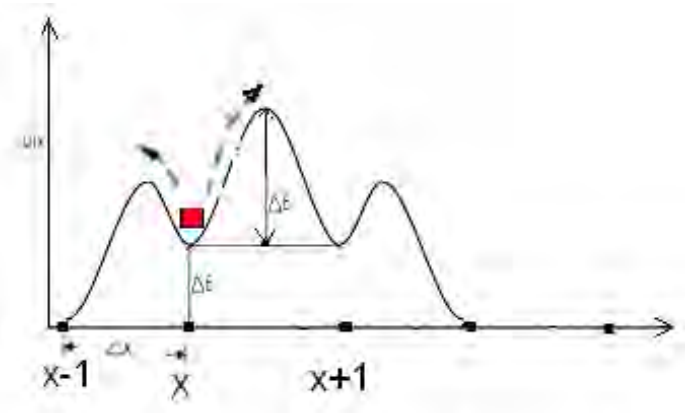

Figure 2.5: The model potential profiles which represents the three different six-jump mechanisms.

barriers to go either forward or backward from one state. To make more simple our model, let us modify this model potential profile in to piece wise linear potential of like Fig 2.6. If we place the vacancy at one particular site and let that site be site (x_2) among those four sites as shown in Fig 2.6, the vacancy will face energy barriers that

it will crosses either to go forward or backward site. Let E_3 be the energy barrier to be crossed by vacancy to go forward and E_2 backward from site(x_2). Now we are in

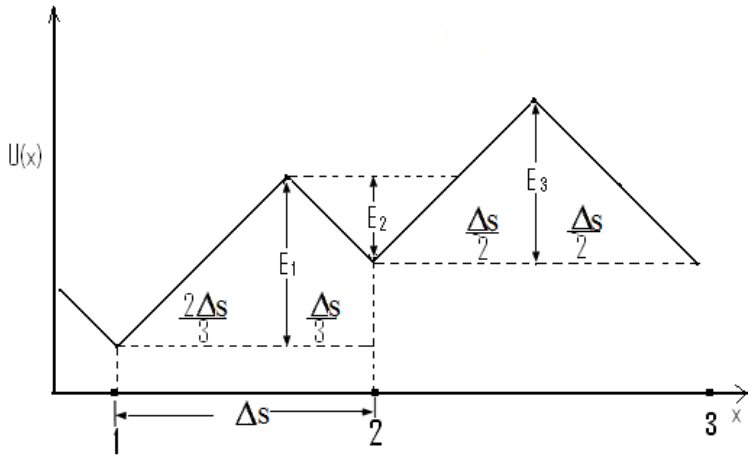

Figure 2.6: linearizing the potential profile and assigning the distance of two consecutive sites as Δs and the barrier heights that the vacancy crosses to go either forward or backward from one site.

a position to calculate the transition rates from the potential profiles of the six-jump mechanism. In that rate equations, the term $U^{'}(x)$ represents the partial derivatives of the potential evaluated at the site x. That means, for this linear potential covering the three sites; x_2, $x_2 \pm \Delta$, the value of $U^{'}(x_2)$ is the slope from x_2 to $x_2 \pm \Delta$. Therefore, the slope that the vacancy will crosse to go either states from state x_2 can be easily calculated as follows

$$U^{'} \mid x_2 \rightarrow x_2 + \Delta = \frac{2}{\Delta s}\frac{E_3}{k_B T}, \qquad U^{'} \mid x_2 \rightarrow x_2 - \Delta = \frac{-3}{\Delta s}\frac{E_2}{k_B T} \tag{2.9}$$

Note that $\Delta = \Delta s$ to represent the distance between each lattice site of six-jump mechanism. If we substitute these slopes in the transition rate equation, we will

obtain the outgoing transition rates of the vacancy from site (x_2) in terms of the energy barrier height.

$$k_6(x_2 + \Delta \mid x_2) = \frac{D_0}{(\Delta s)^2} e^{-\frac{E_3}{k_B T}} \tag{2.10}$$

and

$$k_6(x_2 - \Delta \mid x_2) = \frac{D_0}{(\Delta s)^2} e^{-\frac{3E_2}{2k_B T}} \tag{2.11}$$

In the same fashion, we can calculate the value of $U^{'}(x)$ as well as the transition rates of the other remaining sites. For instance, both the forward and backward transition rates from the first site is given by

$$k_6(x_1 \pm \Delta \mid x_1) = \frac{D_0}{(\Delta s)^2} e^{-\frac{3E_1}{4k_B T}} \tag{2.12}$$

However, for the site x_3 as we may see from Fig 2.6, its transition rates are similar to site x_2 but in the opposite direction. The vacancy crosses E_2 to transit forward and E_3 backward from site x_3. Then the two transition rates are

$$k_6(x_3 + \Delta \mid x_3) = k_6(x_2 - \Delta \mid x_2) = \frac{D_0}{(\Delta s)^2} e^{-\frac{3E_2}{2k_B T}} \tag{2.13}$$

and

$$k_6(x_3 - \Delta \mid x_3) = k_6(x_2 + 1 \mid x_2) = \frac{D_0}{(\Delta s)^2} e^{-\frac{E_3}{k_B T}} \tag{2.14}$$

where

- $k_6(x_i + \Delta \mid x_i)$ - the forward transition rate from site(x_i) for the six jump mechanisms and

- $k_6(x_i - \Delta \mid x_i)$ - the corresponding backward transition rate from that site

2.3.2 Next nearest neighbor mechanism(NNN)

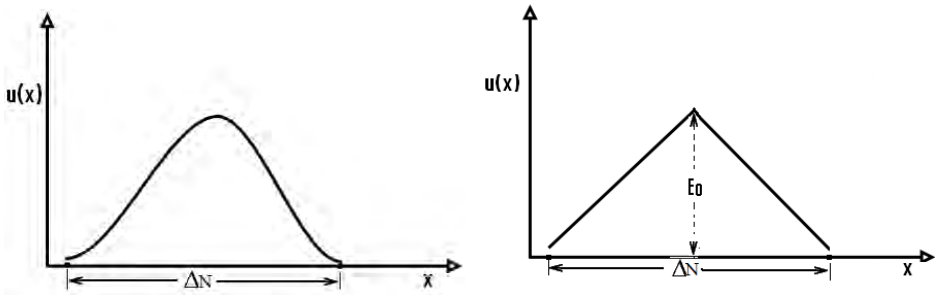

(a) (b)

Figure 2.7: (a) The activation energy of a Ni vacancy in NNN mechanism and (b) its potential profile in linear form.

In next nearest neighbor (NNN) vacancy diffusion mechanism, the vacancy has to make a single jump over the nearest site to the same sublattice. During each cycle the vacancy jumps a distance of lattice size (ΔN) by crossing its potential profile which can be represented by a model potential profile U(x) as shown in Fig 2.7(a). We approximate this model potential profile to the one shown in Fig 2.7(b) which is piece-wise linear potential. In this figure, E_0 is the energy barrier to be crossed by the vacancy to jump forward or backward from one site while ΔN is the lattice spacing between adjacent sites. From this piece-wise linear potential, one can calculate the transition rates of this mechanism. Then the forward and backward transition rates of NNN mechanism from any site is given by

$$k_0(x_i \pm \Delta \mid x_i) = \frac{D_0}{(\Delta N)^2} e^{-\frac{E_0}{k_B T}} \tag{2.15}$$

Where

- $k_0(x_i \pm \Delta \mid x_i)$ - the forward and backward transition rate of this NNN mechanism.

2.3.3 Triple defect mechanism

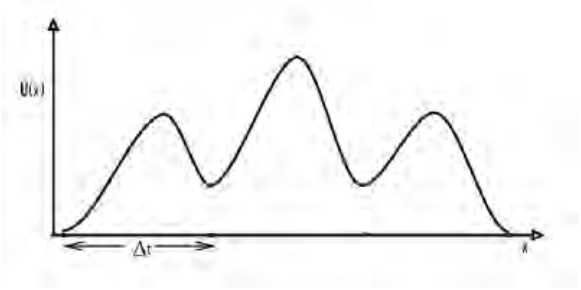

(a)

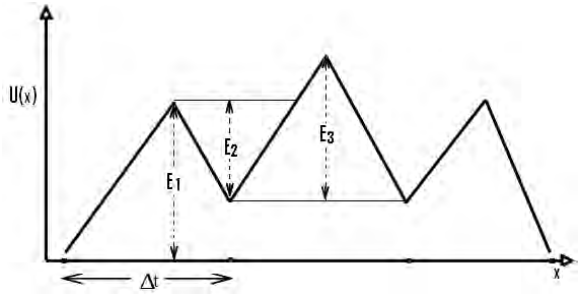

(b)

Figure 2.8: (a) The activation energy of a Ni vacancy in triple defect mechanism and (b) its potential profile in linear form.

In triple defect mechanism, the two vacancies will complete their cycle with four lattice sites and the potential profile of this mechanism calculated by [11] is shown in chapter one. Let us take Fig 2.8(a) as a model potential profile which represent the real potential of this mechanism. We follow the same procedure that we have

done for the first two mechanisms first by discritizing this model potential profile into Fig 2.8(b) which is piece-wise and linear and then calculate each state transition rates along its path. If we start with the first site, the vacancy should cross E_1 to go either forward or backward but if it is at site two it should cross E_3 to go forward and E_2 backward. Therefore, the transition rates for site x_1 are

$$k_t(x_1 \pm \Delta \mid x_1) = \frac{D_0}{(\Delta t)^2} e^{-\frac{3E_1}{4k_BT}} \tag{2.16}$$

Similarly, at site x_2 the out going rates are

$$k_t(x_2 + \Delta \mid x_2) = \frac{D_0}{(\Delta t)^2} e^{-\frac{E_3}{k_BT}} \tag{2.17}$$

$$k_t(x_2 - \Delta \mid x_2) = \frac{D_0}{(\Delta t)^2} e^{-\frac{3E_2}{2k_BT}} \tag{2.18}$$

In site three, as we may see from Fig 2.8(b), it is identical to site x_2 but in the opposite direction. The vacancy crosses E_2 to transit forward and E_3 backward from site x_3. Then the two transition rates are

$$k_t(x_3 + \Delta \mid x_3) = k_t(x_2 - 1 \mid x_2) = \frac{D_0}{(\Delta t)^2} e^{-\frac{3E_2}{2k_BT}} \tag{2.19}$$

$$k_t(x_3 - \Delta \mid x_3) = k_t(x_2 + 1 \mid x_2) = \frac{D_0}{(\Delta t)^2} e^{-\frac{E_3}{k_BT}} \tag{2.20}$$

where

- $k_t(x_i + \Delta \mid x_i)$ - the forward transition rate from site(x_i) for the six jump mechanisms and
- $k_t(x_i - \Delta \mid x_i)$ - the corresponding backward transition rate from that site

Therefore, from such linearized potential profiles, one can calculate easily the transition rates in terms of the potential $U(x)$. Actually all those rate expressions are not only a function of potential $U(x)$ (local energy barrier height) but also they are a function of lattice space Δ, background temperature (k_BT) and diffusion coefficient D_0. To get the actual values of each state transition rates along these diffusion mechanisms, one should substitute values of these parameters. The lattice space, Δ, of these mechanisms are as follows:

- For NNN mechanism, the value of ΔN is is equal to $2.9\hat{A}$
- For the triple defect, $\Delta t = \Delta N\frac{\sqrt{3}}{2} = 2.5\hat{A}$ and
- For the different six-jump mechanisms, $\Delta s = \Delta N\sqrt{2} = 4.101\hat{A}$.

Table 2.1: The local and overall energy barrier height and the diffusion coefficient of the three different six-jump mechanisms that is calculated by [11].

Mechanism	$E_1(ev)$	$E_2(ev)$	$E_3(ev)$	$E_{O.all}(ev)$
Six[110]	2.34	0.33	0.56	2.58
Six[100]st	2.87	0.68	1.55	3.74
Six[100]bent	2.87	0.68	1.41	3.60

Table. 2.1 and Table 2.2 shows the local, overall energy barrier heights and the diffusion coefficient of the three different six-jump mechanisms and the other two remaining mechanisms respectively. One can see from these tables that the vacancy

Table 2.2: The local and overall energy barrier heights and the free diffusion coefficient of the six-jump[110] and the remaining two mechanisms.

Mechanism	$E_1(ev)$	$E_2(ev)$	$E_3(ev)$	$E_{O.all}(ev)$	$D_0(10^{-5}m^2s^{-1})$
NNN	-	-	-	2.58	2.71
Six[110]	2.34	0.33	0.56	2.58	2.77
Triple	0.89	0.59	0.74	1.07	3.45

will crosse different local as well as global energy barrier heights except the NNN mechanism for which the local and overall energy is the same.

These local and overall energy variation will varies the transition rate and one may not have a specific transition rate of each mechanism along its different lattice sites. Because of these energy barrier height variations, we have taken the overall energy to represent each of them and vary the temperature from 1200 to 1500K to see their relation with temperature. Note that this temperature range that we have taken is the temperature range where experimental data for NiAl are found. Fig. 2.9(a) compares the transition rates of the three different six-jump mechanisms in the above temperature intervals. It can be clearly seen that all of them increase with temperature, however, both [100] straight and bent jump rate is lower than [110] six-jump at all temperature. At high temperature (relative to our range), six [100] bent has nearly the same value of that of six[110]. In general, we can conclude that [110] six-jump at all temperature and six [100] bent at high temperature are a favorable path for vacancy diffusion in NiAl among these different six-jump mechanisms.

We have taken the favorable [110]six-jump to represent the collective six-jump mechanisms and compared with the others as shown in Fig. 2.9(b). The figure shows how the transition rates of these three main vacancy diffusion mechanisms in the above temperature range. Even though all of them increase with temperature, the triple

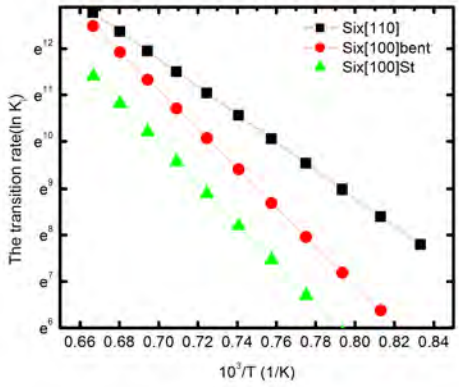

(a)

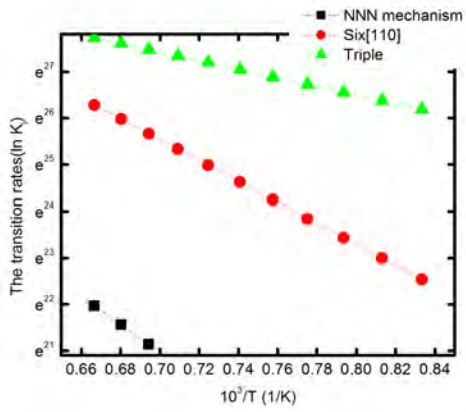

(b)

Figure 2.9: (a)The transition rate as a function of temperature of the the three different six-jump mechanisms (b) The NNN and six-jump and triple defect mechanisms with the corresponding parameters in Table. 2.2.

defect mechanism has the highest rate of all the other mechanisms at any temperature intervals. At high temperature, all of them may contribute for vacancy diffusion but at low temperature both the six [110] and triple mechanisms may contribute for vacancy diffusion. As a whole, six-jump [110] and triple mechanisms are favorable

vacancy diffusion paths especially the triple defect is the most favorable path for vacancy diffusion in NiAl even at low temperature. Besides all of these, usually it is assumed that the temperature dependence of $k(x \pm \Delta \mid x)$ (rates) should follow the Arrhenius law. From these two figures, we report the Arrhenius plot of transition rates in the above temperature range showing that our result obeys this law in the above temperature intervals.

2.4 Simulation of master equation

In section 2.2, I described the time evolution of the vacancy in any of those diffusion mechanism by the master equation, Eq. 2.5. One of the most useful quantities that we can calculate from this master equation is the average time that the vacancy takes to reach a particular site for the first time. This quantity can be determined from a master equation by imposing an absorbing boundary at particular state which will be the last state of each mechanism. The simulation of this Master equation and those transition rate equations can be performed by Artur B. Adib Algorithms [1]. As you have seen in the introduction part, this algorithm is developed to calculate a first passage time of Brownian particle in discrete lattice space and continuous time form instead of the usual method where one consider continuous space and discrete time in solving the Langevin equation. In general this algorithm allows us a discrete space and continuous time simulation of any system. As we may see in the first figure, Adib realization of the fist passage time problem of Brownian particle represents a random walk that exactly represents the distribution of the master equation.

2.4.1 Adib's Algorithm Summary

R. Adib has developed a first passage time algorithm of Brownian particle in discrete lattice space and continuous time form where his algorithm can be summarized as follows;

1. **Initialization:** Initialize the number of lattice sites in the system, rate constants, and random number generators.

2. **Monte Carlo Step:** Generate random numbers to determine the next site

to occupied as well as the time interval. The probability of a given site to be chosen is proportional to the number of neighbor lattice sites.

3. **Update:** Increase the time step by the randomly generated time in Step 2. Update the position of the vacancy based on the chosen site that occurred.

4. **Iterate:** Go back to Step 1 unless the vacancy touches its last lattice site (absorbing boundary).

In general, according to this method:

- *First*, one starts in a given vacant site x_i and calculates the sum of the outgoing rates which will be the propensity function [7]

$$k_{sum}(x_i) = \sum_{x_i^{'}=1}^{n} k(x_i^{'} \mid x_i) \tag{2.21}$$

- *Second*, the time step that the next jump will occur is calculated by selecting an exponentially distributed random number and dividing it by the sum of the propensities. i.e,

$$< \tau >= -\frac{\ln(u_1)}{k_{sum}(x_i)} \tag{2.22}$$

where u_1 a uniform random number generated from U(0, 1). Note that in all our programs, we are going to use *mersenne twister* random number generator. To draws an exponentially distributed random number from a uniform random number *see appendix A*.

- *Third*, a decision is made among the nearest neighboring sites that the vacancy is going next by multiplying a uniformly distributed random number u_2 by the total sum of the propensities. i.e,

$$\frac{k(x_i - \Delta \mid x_i)}{k_{sum}(x_i)} < u_2 \leq \frac{k(x_i + \Delta \mid x_i)}{k_{sum}(x_i)} \tag{2.23}$$

  where

- u_2 another uniform random number generated from U(0,1)

- *Finally*, update the state of the vacancy position according to the above selection to

$$x_i = x_i \pm \Delta \tag{2.24}$$

  and increase the time with

$$t = t + \tau. \tag{2.25}$$

Running this procedure again and again, one can produce (generate) sample trajectories of the ME or the vacancy evolution with its time. Let us set some parameters for the simulation of our model. The rate equations as we see above, is a function of energy (E), temperature (T), the free diffusion coefficient (D_0) and lattice space (Δ_i). We have set these Δ_i for each different mechanisms previously. Next let us set the other parameters as follows

1. The number of lattice points that the vacancy allowed to visit is N = 3 for all mechanisms.

2. The background temperature T = 1200.0K. and

3. Table 2.3 for the local as well as the global energy barrier height and free diffusion coefficient of the three mechanisms

Table 2.3: The local energy barrier heights and diffusion coefficients of the three different mechanisms calculated by [11].

Mechanism	$E_1(ev)$	$E_2(ev)$	$E_3(ev)$	$D_0(10^{-5}m^2s^{-1})$
NNN	2.58	-	-	2.71
Six[110]	2.34	0.33	0.56	2.77
Triple	0.89	0.59	0.74	3.45

In this table, E_0 is the energy barrier to be crossed by the vacancy to go both forward and backward from any site in NNN mechanism. E_1, E_2 and E_3 are the local energy barriers to be crossed by the vacancy through six-jump and triple defect mechanisms. In general, to calculate the mean first passage time along the path of each diffusion mechanisms, we place the vacancy at one particular place as shown in Fig. 2.10 and then apply the following procedures.

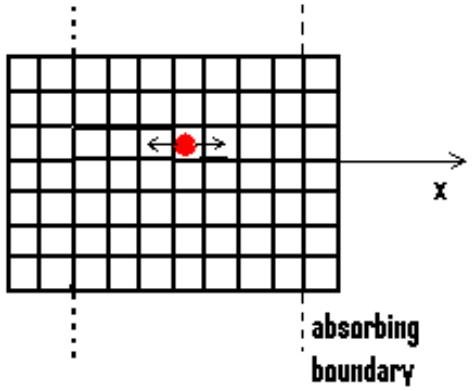

Figure 2.10: In a two dimensional lattice site, a vacancy placed at one point and it can move according to its arrows until it touches its absorbing boundary.

Listing 2.1 Adib Algorithm, Diffusion of a vacancy in one dimension.

Initialization Set the initial position of the vacancy x = 0.0 and place the absorbing site at $x = x_N = 3$ for all mechanisms.
do While $x \leq x_N$
do i = 1, n

$$k_{sum}(x_i) = \sum_{x^{'}=1}^{n} k(x^{'} \mid x)$$

call random number(u_1)

$$\tau_i = -\frac{\ln(u1)}{k_{sum}(x_i)}$$

call random number(u_2)

$$\text{If} \qquad u_2 \leq \frac{k(x_i + \Delta \mid x_i)}{k_{sum}(x_i)}$$

Update the state according to

$$x_i = x_i + \Delta.$$

$$\text{Else if} \qquad u_2 > \frac{k(x - \Delta \mid x)}{k_{sum}(x_i)}$$

$$x_i = x_i - \Delta.$$

Else

$$x_i = x_i.$$

End if
and time of the system updated to

$$t_i = t_i + \tau_i$$

end do

end do while

2.5 Simulation Results

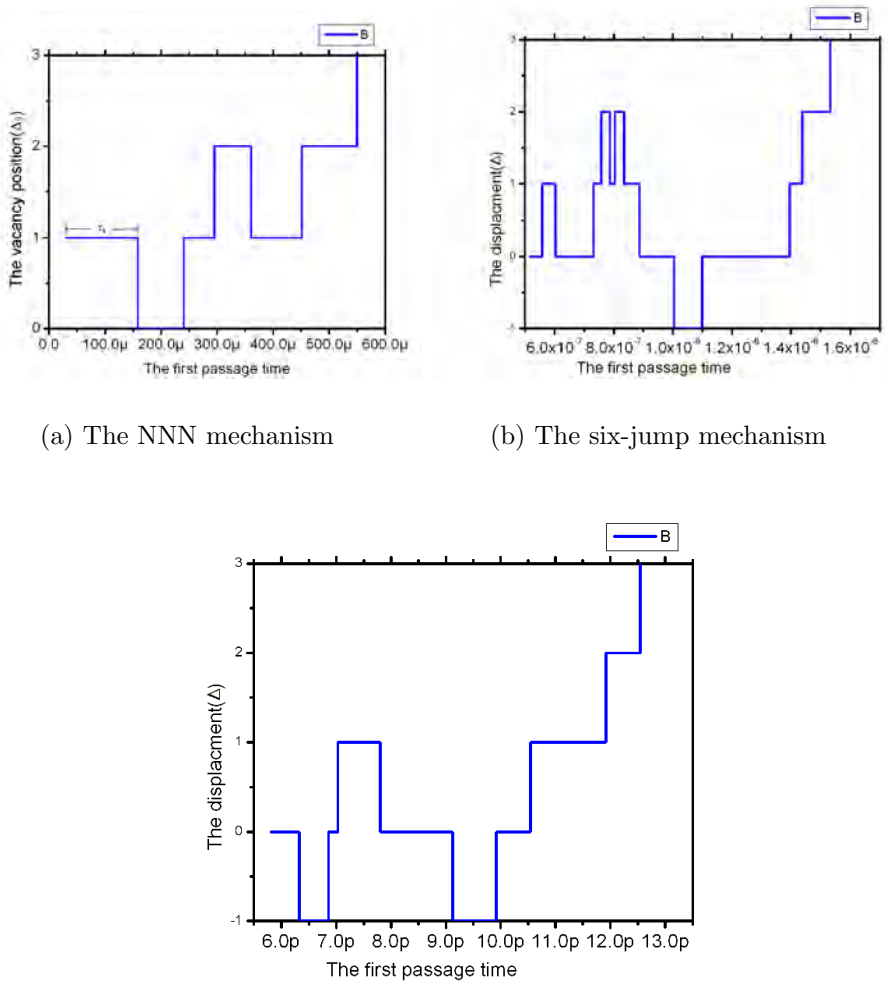

(a) The NNN mechanism

(b) The six-jump mechanism

(c) The triple mechanism

Figure 2.11: The one dimensional trajectory of vacancy motion which illustrates a first passage time taken by the vacancy from x = 0 to the absorbing boundary at x = $3\Delta'$ of the NNN, six-jump and triple defect mechanisms.

The whole process except the initialization is repeated as many times as necessary until the vacancy touches the absorbing states of the three mechanisms for the first

time. In short, according to Adib Algorithm, one should place the vacancy in one of the available states (x_i) of the mechanism and draws an exponentially distributed random number τ_i with mean equal to Eq. 2.22 then jumps to the next state ($x_i \pm \Delta$) that is chosen with probability, Eq. 2.23. The vacancy then moves to this chosen site and the procedure above is repeated until it reaches an absorbing site.

During this process, the position (x_i) and time (τ_i) of the vacancy at each step until it completes each mechanisms are recorded. Figs. 2.11(a), 2.11(b) and 2.11(c) show the position of the vacancy versus the time of the NNN, six-jump and triple defect mechanisms respectively. It can be clearly seen that all trajectories are continuous in time and discrete space where their discreetness in space are labeled with $x = 0\Delta$, 1Δ, $2\Delta \cdots$ and they also show the distance between the two consecutive sites. Note that at each state (x_i), the vacancy waits a random time τ_i which is called the local first passage time required by the vacancy to transit from state x_i to the next state $x_i \pm 1$. Therefore, the total first passage time taken by the vacancy is then the sum of the first local passage times $\tau(x_i)$ from state x_i to the next state $x_i \pm \Delta$. In general, these trajectories are identical with B. Adib [1] of Fig. 2.1, blue discrete line.

The average first passage time taken by the vacancy to reach the absorbing sites of each mechanisms are also simulated by Adib's method using the equation, Eq. 2.2. The following Figs. 2.12(a), 2.12(b) and 2.12(c) show, the mean first passage time taken by the vacancy to reach the absorbtion sites of the NNN, six-jump and triple defect diffusion mechanism computed by this similar method. From these figures, we can see that the mean first passage time taken by the vacancy to complete each of these mechanisms as follows.

- $< \tau_N >= 3.2762 \times 10^{-04}$ sec for the NNN mechanism

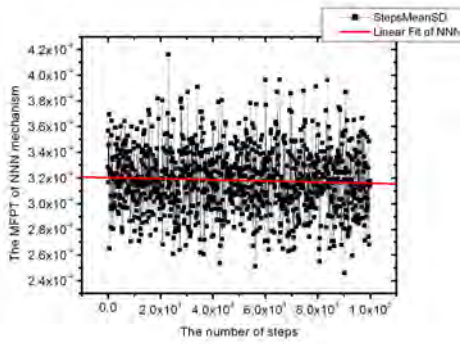

(a) The NNN mechanism

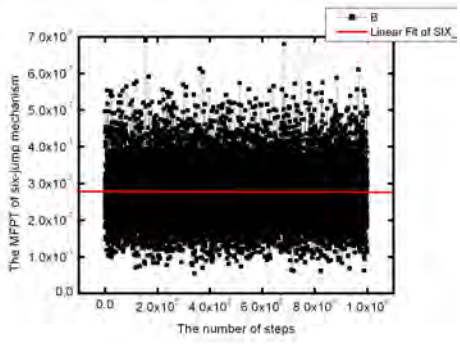

(b) The six-jump mechanism

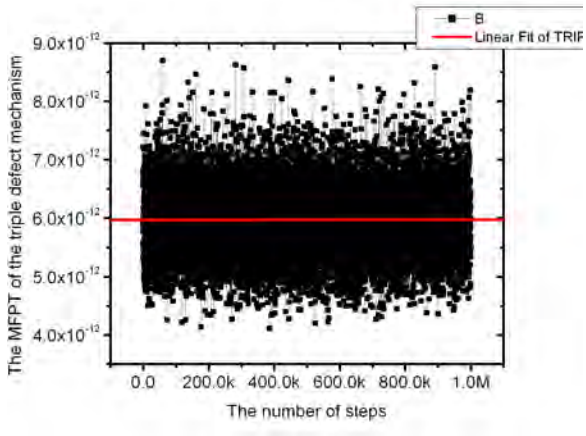

(c) The triple mechanism

Figure 2.12: The mean time, $< \tau_N >$,$< \tau_s >$, and $< \tau_t >$ taken by a vacancy to complete its NNN, six-jump and triple defect mechanisms. 1000,000 samples were taken.

- $< \tau_s >= 3.031554 \times 10^{-07}$ sec for the six-jump mechanism and
- $< \tau_t >= 5.509186 \times 10^{-12}$ sec for the triple defect mechanism.

At the same time the standard deviation $\sigma = \sqrt{< (\tau_i)^2 > - < \tau_i >^2}$ and their ratio $R = \frac{\sigma}{<\tau_i>}$ also known as the relative error of these mechanisms are calculated and

their values are shown below

- $\sigma_N = 1.4971 \times 10^{-04}$ sec and $R_N = 0.4569$ for the NNN mechanism
- $\sigma_s = 5.77492 \times 10^{-07}$ sec and $R_6 = 1.9049$ for the six-jump mechanism and
- $\sigma_t = 3.283745 \times 10^{-12}$ sec and $R_t = 0.59604$ for the triple defect mechanism.

As we see from our result, when the vacancy diffuse via the three vacancy diffusion mechanisms, it takes less time to complete the triple defect and large time to complete its NNN mechanism. In general, this simulation result predict that the triple defect mechanism is the one which contributes more to vacancy diffusion in NiAl compound than the others.

All the three vacancy diffusion mechanisms are simulated from transition rates which are a function energy and temperature. So let us take one of the vacancy diffusion mechanisms which is the Next nearest neighbor(NNN) and see its mean first passage time as a function of energy and temperature. First let us start the effect of energy barrier height in this diffusion mechanism by taking the background temperature at T = 1200.0K and the free diffusion constant of the NNN mechanism, $D_0 = 2.71 \times 10^{-5} m^2.s^{-1}$, we vary the energy from (E =1.0 ev to 4.0 ev) with 0.2 interval. The plot 2.13 shows the MFPT as a function of energy for this diffusion mechanism. As you see from this figure, the MFPT increase with energy, indicating that the vacancy spent more of its time in one lattice point(wells) before it jumps to the next state. Then we can conclude that when the height of the energy barrier that the vacancy crosses becomes large then the MFPT taken by the vacancy becomes longer. In general, the barrier heights that the vacancy crosses influence the mean first passage time as well as the diffusion process of the vacancy in NiAl compound.

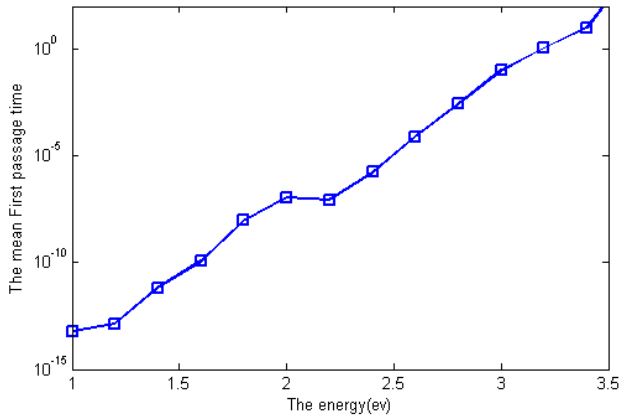

Figure 2.13: The mean first passage time of the vacancy to reach the absorbing state with different energy levels.

Secondly, let us see the effect of temperature on the MFPT by taking the energy at one point, which is the overall energy barrier height $E = 2.58(ev)$. We vary the temperature from 1200.0K to 1500.0K. One can see from the Fig. 2.14 that the mean

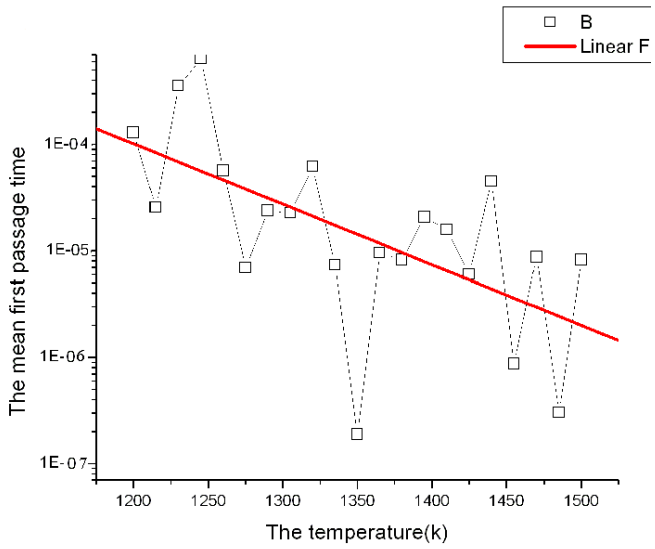

Figure 2.14: The mean first passage time of the vacancy to reach the absorbing state at different temperature.

first passage time decrease as the temperature increase. This is because, when the background temperature is high, the vacancy takes less time at each lattice site. In other word, when the background temperature is high, the vacancy can easily cross the barrier height on those vacancy diffusion mechanisms of NiAl compound.

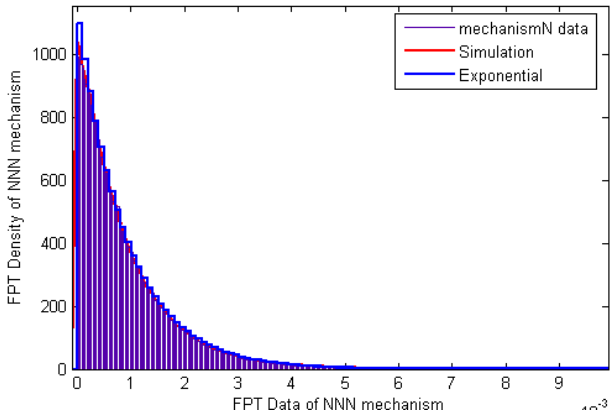

Figure 2.15: The probability distribution function (PDF) of first passage time of the vacancy to reach the absorbing state.

The probability distribution function (PDF) of the first passage time is the rate of change of the vacancy site occupation probability. And from our the numerical simulation we have got the following plot. It shows the probability density function of FPT plotted for many jumps, binned in equal, regularly-spaced interval.

Chapter 3

The mean first passage time and effective diffusion coefficient

3.1 Introduction

In this chapter, we are going to deal with the problem of the mean first passage time and effective diffusion coefficient of the vacancy when it diffuse in NiAl binary alloy via those three main vacancy diffusion mechanisms. In the first section, we formulate the basic mathematical concepts that will handle the three postulated diffusion mechanisms of a vacancy in NiAl. In the second section we calculate the local mean first passage time taken by the vacancy to jump from one lattice site to the next in terms of the jump probabilities p (probability per unit time to jump forward) and q (the jump probability per unit time to jump backward). Finally, we will calculate vacancy's effective diffusion coefficient when it diffuse in those different diffusion mechanisms.

3.2 Motion of a vacancy as a random walk on a lattice

The simple and best model for describing stochastic processes is to consider their motion as a random walk on a one dimensional lattice. This model of random walk

on a lattice captures most of the basic essence of stochastic process. Due to this, numerous dynamical processes in nature can be successfully modeled as a random walk. The first known physical example is the Brownian motion of a small particle immersed in a medium. Secondly, many transport phenomena in solids (e.g. hopping conductivity) are modeled by random walks where the random walk is restricted on a lattice. As previously mentioned in chapter one, in all vacancy diffusion mechanisms, the vacancy jumps from site to site by crossing a certain energy barrier heights in a crystalline structure of NiAl compound. Therefore, the different vacancy diffusion mechanisms that we have mentioned can be modeled as the motion of a Brownian particle over rugged and periodic potential in discrete lattice space.

To look at the details of how long the vacancy takes to move through such a crystal structure of NiAl by crossing that rugged periodic potential, we use the mean first passage time(MFPT) determination technique formulated by I. Goldhirch and Y.Gefen [8]. Before we applying this technique to our problem, we should familiarize ourselves to its basic ideas and parameters. To start with, first we derive the MFPT of a particle moving on a straight line segment. Let us consider a straight line segment with N+1 number of points as shown in the Fig. 3.1. Let p_i be the probability per unit time that the walker jumps from i to i+1 and q_i be the probability per unit time that the walker jumps from i to $i-1$. Obviously, $p_i + q_i \leq 1$, as the walker has the probability to stay at i. As far as the walker is confined to move within the segment, $p_N = q_0 = 0$. The probability to stay at a given initial point i in a single time step is $(1 - p_i - q_i)$. After n consecutive steps the probability to stay at the same initial point i is $(1 - p_i - q_i)^n$. Then let us define the corresponding generating function $\chi(\phi)$, which is defined by,

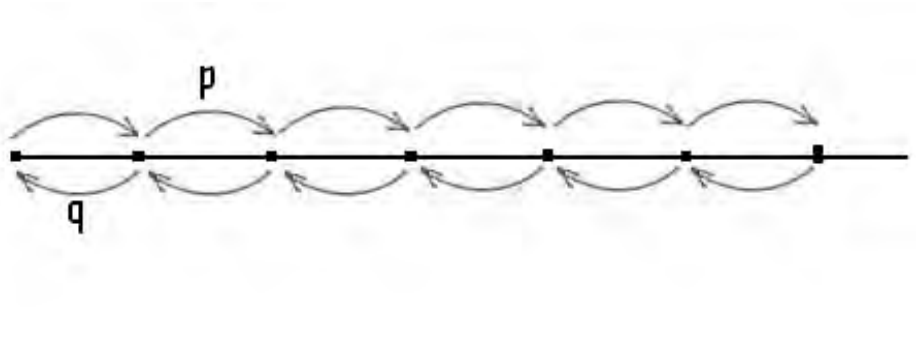

Figure 3.1: Random walk on a striaght segment

$$\chi(\phi) = \sum_{n=0}^{\infty} (1-p-q)^n \exp(in\phi) \tag{3.1}$$

The value of $\chi(\phi)$ simplifies to

$$\chi(\phi) = \frac{1}{1-(1-p-q)\exp(i\phi)} \tag{3.2}$$

In general, if $P(n)$ denotes the probability to perform a given walk in n steps, then the corresponding generating function $\tilde{P}$ is defined as:

$$\tilde{P}(\phi) = \sum_{n=0}^{\infty} P(n) \exp(in\phi) \tag{3.3}$$

Before we go to the detail of the whole process, first lets define two more basic functions.

1. Let T(n) be the probability of the walker to start at the point i = 0, leave it on the first step and reach i = N for the first time without having returned to i =

0 in the process. The corresponding generating function $\tilde{T}(\phi)$ can be expressed as

$$\tilde{T}(\phi) = \sum_{n=0}^{\infty} T(n) \exp(in\phi) \tag{3.4}$$

2. Let Q(n) be the probability of the walker to leave i = 0 in its first step and return to i = 0 in n steps with out having reached to i = N with the associated generating function $\tilde{Q}(\phi)$,

$$\tilde{Q}(\phi) = \sum_{n=0}^{\infty} Q(n) \exp(in\phi) \tag{3.5}$$

Generating functions defined above can be added and multiplied like regular probabilities, except that one does not have to keep track of the order of steps. Our aim is to determine the average time required by the random walker to reach i = N for the first time starting from i = 0. This time is usually called Mean First Passage Time (MFPT), highly related to the probability $P_w(n)$ that the walker reaches i = N for the first time starting from i = 0. The generating function $G(\phi)$ corresponding to $P_w(n)$ is,

$$G(\phi) = \sum_{n=0}^{\infty} P_w(n) \exp(in\phi). \tag{3.6}$$

The MFPT can then be defined as,

$$\tau = \frac{\sum_{n=0}^{\infty} nP_w(n)}{\sum_{n=0}^{\infty} P_w(n)}, \tag{3.7}$$

Which can be also expressed in terms of the probabilities as

$$\tau = \frac{1}{G(\phi)} \frac{dG(\phi)}{di\phi}|_{\phi=0}. \tag{3.8}$$

3.3 Calculation of MFPT for a vacancy diffusing via different mechanisms

Using the above Mean First Passage Time (MFPT) determination techniques, we can calculate the MFPT of a vacancy when it diffuse through the Six-Jump, Triple defect and Next Nearest Neighbor(NNN) mechanisms analytically. As we have seen in the previous section, before MFPT calculation of any stochastic system, it is better to propose some simplified models that can describe the system. Our systems, the three different vacancy diffusion mechanisms, are then modeled as motion of a vacancy in one dimensional discrete lattice sites where the vacancy jumps from site to site by crossing that rugged potential profiles. For such kind of vacancy dynamics and potential profiles. Simply the model we propose is a one dimensional motion of a vacancy along the single path.

3.3.1 Six-jump mechanisms

Recent studies [11, 21] of the six-jump mechanisms predict that the minimum energy path (the energy profile) of the different six jump mechanisms consists of three atomic transitions not six as it was thought before [3]. As an example, the potential profile

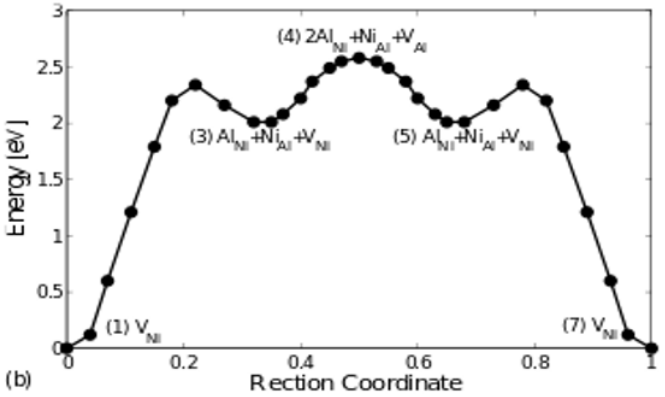

Figure 3.2: The minimum energy path of [110] six-jump cycles

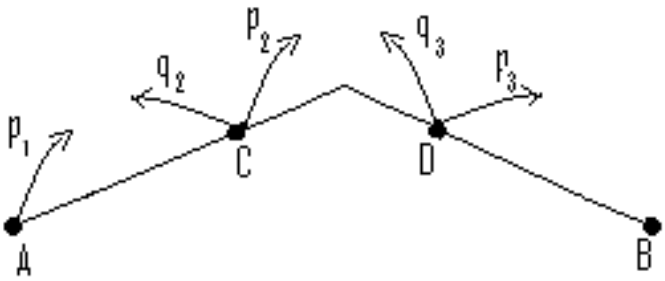

Figure 3.3: Random walk on a bent segment. At each point there is a probability per unit time to go forward and backward

of one of the six-jump mechanism, six [110] calculated by [11] is shown in Fig. 3.2. The motion of a vacancy in a lattice and for such kind of energy profile, can be taken as the motion of a vacancy through one of the paths indicated in the Fig. 3.3, which is the same as a random walk on a single bent segment. These four lattice sites represent the stable and meta-stable states of the three jump points and as you see at

each lattice point, we have a corresponding jump probabilities p_i and q_i. Let $P_w(n)$ be the probability that the vacancy reaches i = B for the first time starting from i = A. The generating function corresponding to $P_w(n)$ be $G_{AB}(\phi)$. In order to get the generating function, $G_{AB}(\phi)$ we need the expression for T_{AB} and Q_{AB} in terms of $\tilde{T}_{AB}(\phi)$, $\tilde{Q}_{AB}(\phi)$ and $\chi_A(\phi)$. These terms on the other hand describes the following process

- A walker at point A can stay there for a number of steps (with ϕ probability $\chi_A(\phi)$),
- Move out of A and return to A without having touched B (with ϕ probability $\tilde{Q}_{AB}(\phi)$), then stay at A and repeat the process a number of times
- Eventually it will start out at A and reach B without returning to A again (with ϕ probability $\tilde{T}_{AB}(\phi)$).

Let us define one more ϕ probability R_A which is the ϕ probability of the vacancy starting at point A, leave A and return to A without touching B. Therefore, the normalized probability at vertex A, $R_A(\phi)$, is given by

$$R_A = \chi_A + \chi_A \tilde{Q}_{AB} \chi_A + \cdots \tag{3.9}$$

One can rearrange Eq. 3.9 and after some algebra

$$R_A = \frac{\chi_A}{1 - \chi_A \tilde{Q}_{AB}} \tag{3.10}$$

This equation refers to all possibilities to start at A and return to it without touching B. This includes the following processes:

- Staying at A for a number of steps ($\chi_A(\phi)$),
- Leaving A and returning to A without reaching D (Q_{AD});
- Leaving A, reaching D at least once, and returning to A (Q'_{AB}).

Therefore, R_A is composed of the above expressions. And among these expressions $\tilde{Q}_{AB}$ is given by

$$\tilde{Q}_{AB} = Q_{AD} + Q'_{AB} \tag{3.11}$$

Where

$$Q_{AD} = T_{AC}\chi_C T_{CA} \tag{3.12}$$

And

$$Q'_{AB} = T_{AD}R_D T_{DA} \tag{3.13}$$

Here R_D is the ϕ probability of the vacancy starting at point D, leave D and return to D without touching B and A. Therefore, the normalized probability at vertex D, $R_D(\phi)$, is given by

$$R_D = \frac{\chi_D}{1 - \chi_D Q_{DA}} \tag{3.14}$$

The last term $\tilde{T}_{AB}$ consists of the ϕ probability to leave A and reach points C and D without ever returning to A, then stay at D or leave D and return to it (without reaching either A or B) unspecified number of times and then leave D towards B without returning to C. It is given by,

$$\tilde{T}_{AB}(\phi) = \tilde{T}_{AD} R_D T_{DB} \tag{3.15}$$

Where

$$\tilde{T}_{AD}(\phi) = \tilde{T}_{AC} \chi_C \tilde{T}_{CD} \tag{3.16}$$

Therefore, finally the ϕ probability, $G_{AB}(\phi)$, of the vacancy to start at A and reach B considering all the realizations is given by

$$G_{AB}(\phi) = R_A(\phi) T_{AB}(\phi) \tag{3.17}$$

The term which explains the process that the vacancy starts at D and leaves D and returning to D without reaching A is given by

$$Q_{DA} = T_{DC} \chi_C T_{CD} \tag{3.18}$$

And the other term is which explains that the vacancy leaves D and reach point C and stay there for a number of steps and then leave C towards A without returning to C. And it is given by

$$T_{DA}(\phi) = T_{DC}\chi_C T_{CA} \tag{3.19}$$

On the other hand, the ϕ probability of the vacancy to make nearest neighbor jumps are

$$\tilde{T}_{AC} = p_1 \exp(i\phi), \tag{3.20}$$

$$\tilde{T}_{CA} = q_2 \exp(i\phi), \tag{3.21}$$

$$T_{CD} = p_2 \exp(i\phi), \tag{3.22}$$

$$T_{DC} = q_3 \exp(i\phi), \tag{3.23}$$

and

$$T_{DB} = p_3 \exp(i\phi) \tag{3.24}$$

The ϕ probability to stay at point A, $\chi_A(\phi)$ is given by

$$\chi_A = \frac{1}{1-(1-p_1)e^{i\phi}} \tag{3.25}$$

While χ_C and χ_D

$$\chi_C = \frac{1}{1-(1-p_2-q_2)e^{i\phi}} \tag{3.26}$$

and

$$\chi_D = \frac{1}{1-(1-p_3-q_3)e^{i\phi}} \tag{3.27}$$

Putting all the required terms in those equations governing the single path model, we find expressions of G_{AB} and then differentiating as

$$\frac{dG_{AB}(\phi)}{di\phi}|_{\phi=0} \tag{3.28}$$

And then multiply

$$\frac{1}{G_{AB}(\phi)}\frac{dG_{AB}(\phi)}{di\phi}|_{\phi=0} = \frac{p_1(p_2+p_3+q_3)+q_2(p_3+q_3)+p_2p_3}{p_1p_2p_3} \tag{3.29}$$

Therefore, the MFPT of a vacancy diffusing in one dimension via one of the Six-Jump cycle through a single path becomes,

$$\tau_s = \frac{p_1(p_2 + p_3 + q_3) + q_2(p_3 + q_3) + p_2 p_3}{p_1 p_2 p_3} \tag{3.30}$$

where

- τ_s - the mean first passage time ,
- p_i - the probability per unit time to go forward from site i and
- q_i- the probability per unit time to go backward from from site i.

3.3.2 Triple defect mechanisms

The triple defect is one of the vacancy diffusion mechanisms in B2 intermetallics. In NiAl, this mechanism consists of four Nearest Neighbor(NN) jumps initiated by two Ni vacancies and a Ni antisite atom see Fig. 1.10(a) in chapter one. Previous

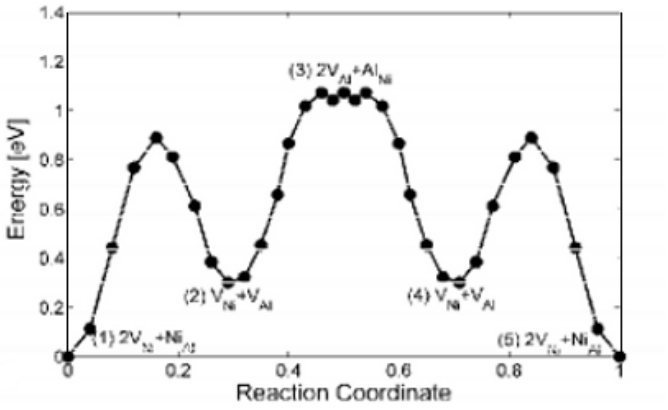

Figure 3.4: The Minimum Energy path of Triple defect jumps

computational work by [11] using First-principles density functional theory in static lattice simulations, predicted that Ni diffusion in NiAl could complete by three step

mechanism. The corresponding minimum energy path (potential profile) of the triple defect mechanisms is shown in the Fig. 3.4 which is calculated by [11] using First-principles density functional theory in static lattice simulations. Even though there is difference in the local energy barrier heights of this mechanism compared with the six-jump one, one can take the same model potential profile as the six-jump cycle. Therefore, we can model the motion of a vacancy in this minimum energy path (rugged and periodic potentials) as a random walk on a single bent segment which is shown in previous section. Then following the same procedure as we have done for six-jump mechanism, one can reach the following mean first passage time expression for triple defect mechanism,

$$\tau_t = \frac{p_1(p_2 + p_3 + q_3) + q_2(p_3 + q_3) + p_2p_3}{p_1p_2p_3} \tag{3.31}$$

where

- τ_t - the mean first passage time taken by the vacancy to complete the triple defect cycle,
- p_i - the probability per unit time to go forward from site i and
- q_i- the probability per unit time to go backward from from site i.

3.3.3 Next Nearest neighbor (NNN) mechanisms

This mechanism consists of Next Nearest Neighbor(NNN) jumps. See the details in chapter one. It is pointed out that a vacancy initially at one corner of a lattice can jump to the next nearest neighbor site of the same species with some probability. It completes its cycle with the following minimum energy path which is shown

Fig. 3.5 [11]. Models that we considered in the previous section are still applicable for

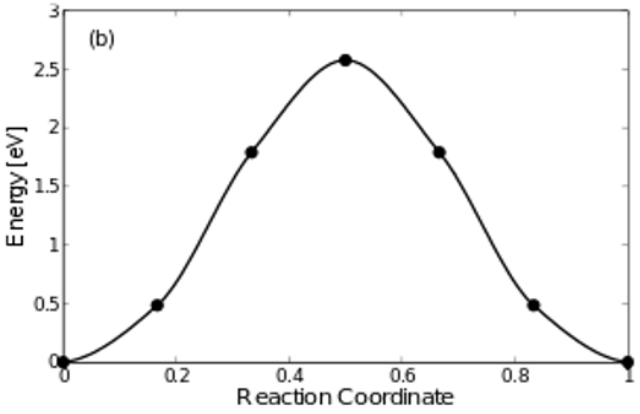

Figure 3.5: The Minimum Energy path of NNN jump

this type of jump too. Assuming that the motion of the vacancy as a random walk on a straight line see, Fig. 3.6, where each point represents a period. Let $p_i = p_0$ be

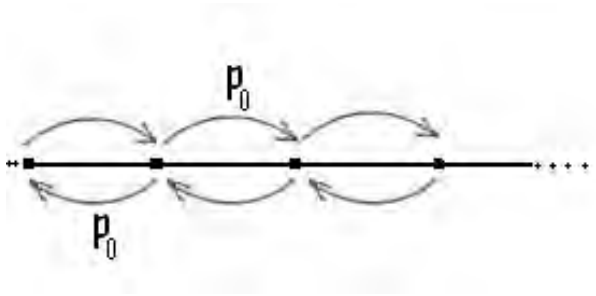

Figure 3.6: Random walks of vacancy diffusion type NNN jump on a straight line

the probability per unit time that the walker jumps from i to i+1 or $i-1$. In other word the probability per unit time that vacancy jump either side is the same. Since, $p_0 + p_0 \leq 1$, as the vacancy has the probability to stay at i. The probability to stay at any initial point i in a single time step is $(1 - p_0 - p_0)$. After n consecutive steps the probability to stay at the same initial point i is $(1 - 2p_0)^n$. Then let us define the

corresponding generating function $\chi(\phi)$, which is defined by,

$$\chi(\phi) = \sum_{n=0}^{\infty} (1-2p_0)^n \exp(in\phi) \tag{3.32}$$

The value of $\chi(\phi)$ simplifies to

$$\chi(\phi) = \frac{1}{1-(1-2p_0)\exp(i\phi)} \tag{3.33}$$

The ϕ probability of the vacancy to make nearest neighbor jumps from i to either side of $i \pm 1$ is given by

$$\tilde{T}_{i\pm1} = p_0 \exp(i\phi), \tag{3.34}$$

In general, if $P(n)$ denotes the probability to perform a given walk in n steps, then the corresponding generating function $\tilde{P}$ is defined as:

$$\tilde{P}(\phi) = \sum_{n=0}^{\infty} P(n) \exp(in\phi) \tag{3.35}$$

The ϕ probability controlling the motion of a vacancy in NNN mechanism through a single path is simply calculated as

$$G(\phi) = \chi_A(\phi) T_{i\pm1} = \chi_A(\phi) p_0 \exp(i\phi) \tag{3.36}$$

From Eqs. 3.33 and 3.34, one obtains:

$$G(\phi) = \frac{p_0 \exp(i\phi)}{1 - (1 - 2p_0)\exp(i\phi)} \tag{3.37}$$

The mean first passage time τ_N to jump from point A to point B, could be calculated as

$$\tau_N = \frac{1}{G(\phi)} \frac{dG(\phi)}{di\phi}|_\phi = 0 = \frac{1}{2p_0} \tag{3.38}$$

where

- p_0 is the probability per unit time for the vacancy to jump both forward and backward from any site and
- τ_N is the MFPT taken by the vacancy to complete one jump

We have derived the expressions of MFPT's as the functions of local jump probabilities for the three proposed vacancy diffusion mechanisms. But these MFPT expressions would not demonstrate the role of parameters such as energy barrier height, the temperature, and the lattice distance. Then in next sections, we are going to calculate the local jump probabilities, p_1, p_2 and p_3 and p_0 as the functions model parameters.

3.3.4 Local Mean First Passage Times and Jump Probabilities

The dynamics of a vacancy in particular of the three different six-jump cycles which is explained in the above sections can be expressed as the diffusion process via succession of the nearest neighbor jumps assumed as the motion of a system in one

dimensional rugged and periodic potential. Considering the high friction limit, This kind of dynamics could be explained with the equation [6] which is given by

$$\frac{\partial p(x,t \mid x_0,0)}{\partial t} = D_0 \frac{\partial \left[\beta U^{'}(x) p(x,t \mid x_0,0)\right]}{\partial x} + D_0 \frac{\partial^2 p(x,t \mid x_0,0)}{\partial x^2} \tag{3.39}$$

where

- $p(x,t \mid x_0,0)$ is the probability density of finding the particle at position x at time t given that it was initially at position x_0.
- $U^{'}(x) = \frac{U(x)}{dx}$ with U(x) being the potential function
- D_0 is the diffusion coefficient and $\beta = \frac{1}{k_B T}$.

This is the forward Fokker-Planck equation. It gives more directly the values of measurable quantities as a function of the observed time t. On the other hand, the backward equation find its application in the study of first passage time and mean exit time problems, in which we find the probability that the particle leaves a region in a given time. Therefore, if the stochastic single jump process between neighboring intermediate states are known then the first passage time of the vacancy should be determined by solving the backward Fokker-Planck equation. Therefore, we are going to use the corresponding backward Fokker-Planck of the above equation which is given by [6]

$$\frac{\partial p(x,t \mid x_0,0)}{\partial t} = -D\beta U^{'}(x) \frac{\partial p(x,t \mid x_0,0)}{\partial x_0} + D \frac{\partial^2 p(x,t \mid x_0,0)}{\partial x_0^2} \tag{3.40}$$

Local Mean First Passage Times

Now let us specify our system by confining the vacancy in the following range

$$a \leq x \leq b \tag{3.41}$$

It might be absorbed or reflected at either end as the case may be. For definite we take a system with

$$\begin{aligned} \text{absorbing barrier at } x &= a \\ \text{absorbing barrier at } x &= b \end{aligned} \tag{3.42}$$

To know the duration of a Brownian particle whose motion is described by the Fokker-Plank equations Eqs. 3.39 or 3.40 remains in the above region of x. The solution of this problem can be achieved by use of the backward FPE. 3.40.
Let $G(x_0, t)$ be the probability of finding the vacancy in the region (a, b) after a later time t initially at x_0. And this can be explained as

$$G(x_0, t) = \int_a^b p(x, t \mid x_0, 0) \tag{3.43}$$

Where

- $p(x, t \mid x_0, 0)$ is the probability of finding the particle at position x at time t

given that it was initially at position x=0.

And $p(x,t \mid x_0,0)$ is governed by the Smoluchowski equation [6], where its corresponding backward Fokker-Plank equation can given by

$$\frac{\partial p(x,t \mid x_0,0)}{\partial t} = -D\beta U^{'}(x)\frac{\partial p(x,t \mid x_0,0)}{\partial x_0} + D\frac{\partial^2 p(x,t \mid x_0,0)}{\partial x_0^2} \tag{3.44}$$

Let take that the system is homogenous in time. Then we can write

$$p(x,t \mid x_0,0) = p(x,0 \mid x_0,-t) \tag{3.45}$$

Hence $G(x,t)$ obeys the equation

$$\frac{\partial G(x_0,t)}{\partial t} = -D\beta U^{'}(x)\frac{\partial G(x_0,t)}{\partial x_0} + D\frac{\partial^2 G(x_0,0)}{\partial x_0^2} \tag{3.46}$$

With the initial conditions

$$p(x,t \mid x_0,0) = \sigma(x - x^{'}) \tag{3.47}$$

G(x,o) becomes

$$G(x,o) = \begin{cases} 1 & a \leq x \leq b \\ 0 & \text{otherwise} \end{cases} \tag{3.48}$$

According to the above boundary condition if the vacancy reaches x=a or x=b it will be absorbed immediately, so the probability or prob($T \geq t$) = 0 when x =a or x=b. Since G(x, t) is the probability that $T \geq t$ the mean of any function of T is

$$< f(T) >= -\int_0^\infty f(t) dG(x,t) \tag{3.49}$$

Then the first passage time will be given by

$$< t >= T(x_0) = -\int_0^\infty t \frac{\partial G}{\partial t} \tag{3.50}$$

and then reduced to

$$T(x_0) = \int_0^\infty G(x_0, t) dt \tag{3.51}$$

Since $G(x_0, \infty) = 0$ note that

$$\int_0^\infty \frac{\partial G(x_0,t)}{\partial t} dt = G(x_0, \infty) - G(x_0, 0) = -1 \tag{3.52}$$

From Eqs. 3.46. and 3.52. we get

$$-D\beta U^{'}(x_0) \frac{\partial T}{\partial x_0} + D \frac{\partial^2 T}{\partial x_0^2} = -1 \tag{3.53}$$

Taking

$$\psi(x) = \exp\left[\int_a^x dx \left(\frac{2A(x)}{B(x)}\right)\right] \tag{3.54}$$

and imposing the boundary conditions

$$T(b) = T(a) = 0 \tag{3.55}$$

Finally solving this equation for T, after some algebra we will get the following expression

$$T(x) = \frac{2\left[\int_x^b \frac{dy'}{\Psi(y')}\int_a^{y'}\frac{\Psi(z)}{B(z)}dz - \int_x^b \frac{dy}{\Psi(y)}\int_a^x \frac{dy'}{\Psi(y')}\int_a^{y'}\frac{\Psi(z)}{B(z)}\right]}{\int_a^b \frac{dy}{\Psi(y)}} \tag{3.56}$$

When we solve this equation using the other two boundary conditions .i.e, suppose the barrier at a is reflecting instead of absorbing and b absorbing as it is. In this case the above expression becomes

$$T(x) = 2\int_x^b \frac{dy}{\Psi(y)}\int_a^y \frac{\Psi(z)}{B(z)}dz \tag{3.57}$$

And in the same fashion when a is absorbing and b reflecting we obtain

$$T(x) = 2\int_a^x \frac{dy}{\Psi(y)} \int_y^b \frac{\Psi(z)}{B(z)} dz \tag{3.58}$$

Now let us apply the above equations in calculating the MFPT of vacancy when it diffuse through those ragged and periodic potentials of the three diffusion mechanisms. Let us start with the six-jump mechanism which has three different types. Since in all the three six-jump mechanisms, the vacancy completes its cycle within four lattice points with the corresponding potential profiles that is shown chapter one. Even though, we may have three different six-jump cycles, let us take one potential profile Fig. 3.7, which represents the collective six-jump mechanisms. To calculate the MFPT

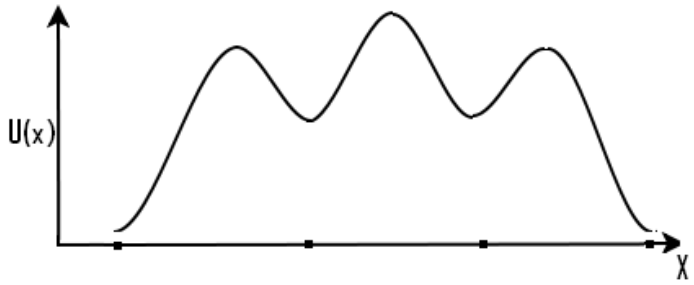

Figure 3.7: Our model potential profile which represent the three different six-jump mechanism.

of the vacancy to jump either forward or backward from a single site, let us take this model potential profile which is not linear. To make more simple our model, we are going to reduce the non-linear potential profile to the one which is assumed to be symmetric, piecewise and linear like of Fig. 3.8 above. Let equations governing the piecewise and linear potential profile of this figure are given by

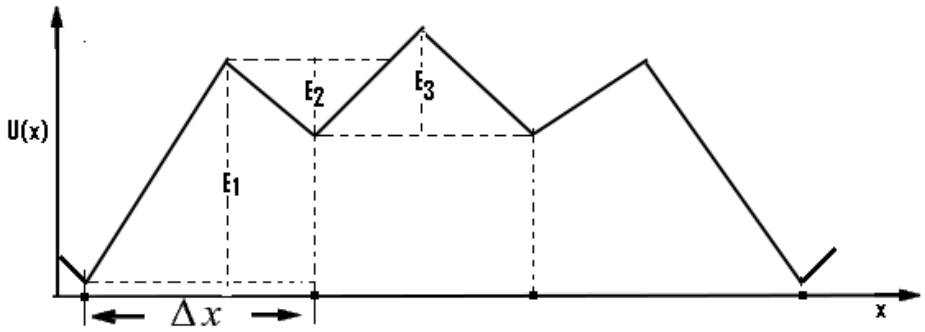

Figure 3.8: Linearizing the model potential of the collective Six-ump mechanism.

$$U(x) = \begin{cases} -\frac{3E_1 x}{2\Delta} & \text{if } x < 0 \\ \frac{3E_1 x}{2\Delta} & \text{if } 0 < x < \Delta \\ 2E_2 + E_1 - \frac{3E_1 x}{2\Delta} & \text{if } \Delta < x < \frac{2\Delta}{3} \end{cases} \tag{3.59}$$

Consider some part of the above linearized potential like of Fig. 3.9 which is asymmetric double well potential. Now we are in a position calculate the MFPT taken by the particle to jump from one well to another. Let the vacancy be at point x = 0. Then using Eqs. 3.57 and 3.58, we can calculate MFPT taken by the vacancy to diffuse from x = 0 to x = Δ and from x = Δ to x = 0, respectively. Let us start in calculating the MFPT from x = 0 to x = Δ, first we have to assume that our reflecting boundary is to the left of x = 0 in the limit $x \to \infty$ and the vacancy is considered to be absorbed at x = Δ. From the definition of $\psi(x)$, inserting the value of A(x) and B(x) from Eq. 3.54. we find

$$\psi(x) = \exp(-\beta U(x)) \tag{3.60}$$

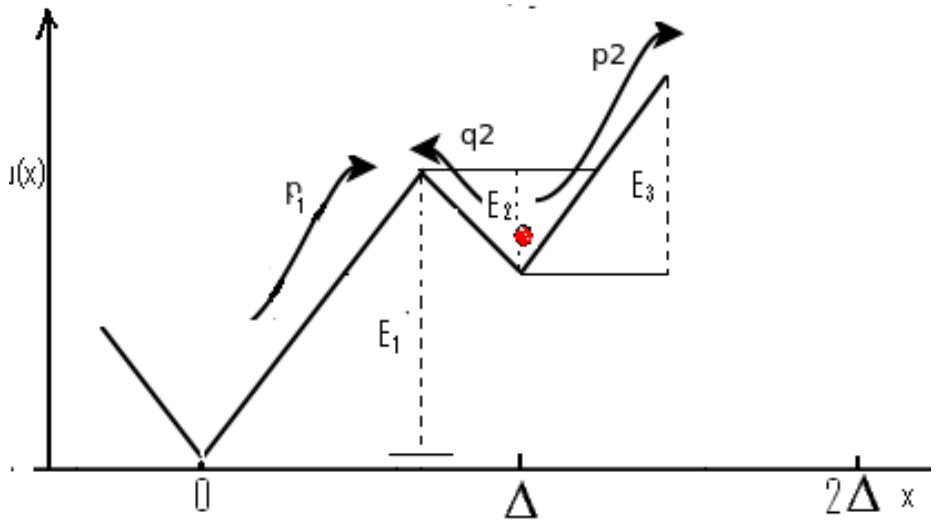

Figure 3.9: Asymmetric piecewise linear double well potential which is a part of the above linearized potential

substitute this value in Eq. 3.57, one obtains

$$T(x) = \frac{1}{D_0} \int_x^{\Delta} dy \exp(\beta U(y)) \int_a^y dz \exp(-\beta U(z)) \tag{3.61}$$

With the substitution of x = 0 and taking the limit $a \to -\infty$,we have thus,

$$T(0 \to \Delta) = \frac{1}{D_0} \int_0^{\Delta} dy \exp(\beta U(y)) \int_{-\infty}^y dz \exp(-\beta U(z)) \tag{3.62}$$

Taking the right values U(y) and U(z) from the potential in Eq. 3.59 and then substitute in the above equation. Finally, when E_1 is large compared to $k_B T$, the above expression takes a simple form

$$T(0 \to \Delta) \simeq \frac{4}{D_0}\left(\frac{\Delta}{\beta(E_1+E_2)}\right)^2 \exp(\beta E_1) \tag{3.63}$$

This is the mfpt taken by the vacancy to diffuse from x = 0 to Δ. Similarly, for the case when the reflecting boundary is to the right of x = Δ and the absorbing boundary is at x = 0, the MFPT will be

$$T(x) = \frac{1}{D_0}\int_{\Delta}^{0} dy \exp(\beta U(y)) \int_{y}^{\infty} dz \exp(-\beta U(z)) \tag{3.64}$$

In this case, our reflecting boundary is to the right of x = Δ and the particle considered to be absorbed at x = 0. The appropriate expression of MFPT for such a situation is Eq. 3.58, with a = 0; x = Δ and the $\Delta \to \infty$, we find

$$T(\Delta \to 0) = \frac{1}{D_0}\int_{\Delta}^{0} dy \exp(\beta U(y)) \int_{y}^{\infty} dz \exp(-\beta U(z)) \tag{3.65}$$

With the same fashion the mfpt taken by the vacancy to diffuse from $x = \Delta$ to x=0 is

$$T(\Delta \to 0) \simeq \frac{4}{D_0}\left(\frac{\Delta}{\beta(E_1+E_2)}\right)^2 \exp(\beta E_2) \tag{3.66}$$

The result of these two equations, Eqs. 3.63 and 3.66 is identical to [22]. From the above Fig. 3.9, you see terms like p_1, p_2 and p_3 which are hopping probability per unit time from one site to its neighbor sites. Assume that the vacancy is placed at

point $x = \Delta$ of Fig. 3.9 and let the probability per unit time of hoping to the right is p_2, and the probability per unit time of hoping to the left is q_2. During this hoping process, the vacancy crosse an energy barriers. E_3 and E_2 are energy barriers that the vacant crosse to go either forward and backward from site $x = \Delta$ respectively. This whole process can be considered a random walk, with step size Δ, i.e. at the large scale it is an effective random walk.

To find an expression of the MFPT in terms of a local jump, we are going to borrow Kramer's rule. According to this rule, for arbitrary time homogenous stochastic process, Kramer's flux-over barrier τ = the rate of escape $(1/\tau)$ is identical to the inverse of the associated mean first passage time. Therefore, the local jump probability, p_1 is equal to the inverse of $T(0 \to \Delta)$. i.e

$$p_1 = \frac{1}{T(0 \to \Delta)} = \frac{D_0}{4}\left(\frac{\beta(E_1 + E_2)}{\Delta}\right)^2 \exp(-\beta E_1) \tag{3.67}$$

Similarly at lattice point $x = \Delta$, there are jumps to either side and these jumps and probabilities are

$$p_2 = \frac{1}{T(\Delta \to 2\Delta)} \tag{3.68}$$

$$q_2 = \frac{1}{T(\Delta \to 0)} \tag{3.69}$$

Where

- $T(\Delta \to 2\Delta)$ -be the first passage time that the vacant takes to go forward starting at point $x = \Delta$ and

- $T(\Delta \rightarrow 0)$ -be the first passage time that the vacant takes to go backward starting at point $x = \Delta$.

With the substitution of the corresponding mfpt expression, we will get

$$p_2 = \frac{D_0}{4}\left(\frac{\beta(E_2 + E_3)}{\Delta}\right)^2 \exp(-\beta E_3) \tag{3.70}$$

$$q_2 = \frac{D_0}{4}\left(\frac{\beta(E_1 + E_2)}{\Delta}\right)^2 \exp(-\beta E_2) \tag{3.71}$$

Finally at point $x = 2\Delta$, the probabilities and jumps times are

$$p_3 = \frac{1}{T(2\Delta \rightarrow 3\Delta)} \tag{3.72}$$

and

$$q_3 = \frac{1}{T(2\Delta \rightarrow \Delta)} \tag{3.73}$$

Let us take Eq. 3.30 which is the MFPT of one of the six-jump cycles and it can be simplified as follows;

$$\tau_s = \frac{1}{p_1} + \frac{1}{p_2} + \frac{1}{p_3} + \frac{q_2}{p_1 p_2} + \frac{q_3}{p_2 p_3} + \frac{q_2 q_3}{p_1 p_2 p_3} \tag{3.74}$$

Due to symmetry of the potential profile of six-jump cycles, there will be only three different jump probabilities, in other word $p_2 = q_3$ and $p_3 = q_2$. Hence the above equation reduces to

$$\tau_s = \frac{2}{p_1} + \frac{1}{p_2} + \frac{2}{p_3} + \frac{q_2}{p_1 p_2} \tag{3.75}$$

If we substitute the local MFPT expressions that we have calculated above instead of the local jump probabilities in this equation, we will obtain;

$$\tau_s = \frac{4}{D_0}\left[2\left(\frac{\Delta}{\beta(E_1+E_2)}\right)^2 \exp(\beta E_1) + 2\left(\frac{\Delta}{\beta(E_1+E_2)}\right)^2 \exp(\beta E_2)\right] + \left[\left(\frac{\Delta}{\beta(E_2+E_3)}\right)^2 \exp(\beta E_3) + \left(\frac{\Delta}{\beta(E_2+E_3)}\right)^2 \exp(\beta(E_1 - E_2 + E_3))\right] \tag{3.76}$$

considering $\exp[\beta(E_1 - E_2 + E_3)]$ as a common term, this equation becomes as follows

$$\tau_s = \frac{4}{D_0}\exp[\beta(E_1 - E_2 + E_3)]\left[2\left(\frac{\Delta}{\beta(E_1+E_2)}\right)^2 \exp[\beta(E_2 - E_3)] + \right] + \left[2\left(\frac{\Delta}{\beta(E_1+E_2)}\right)^2 \exp[\beta(E_2 - E_1)] + \left(\frac{\Delta}{\beta(E_2+E_3)}\right)^2 \exp[\beta(2E_2 - E_3 - E_1)]\right] + \left[\left(\frac{\Delta}{\beta(E_2+E_{32})}\right)^2\right] \tag{3.77}$$

To reduce this equation into a simple form, let us take one of its parameters, energy, in to consideration. As shown in the above Fig. 3.8, within one complete six-jump mechanism, there are three local energy barrier heights where the vacancy will cross: E_1 to jump both forward and backward from the first site, E_3 to go forward and E_2

backward from second site and due to symmetry the reverse is true for site three. Let us draw this energy configuration again like shown in Fig. 3.10, E_1 and E_3 are upward and E_2 is downward. The over all energy barrier height crossed by the vacancy to complete one six-jump mechanism can be approximated from its local ones and let that be

$$E_{gs} = E_1 - E_2 + E_3 \tag{3.78}$$

where

- E_{gs} is the overall energy barrier height within a one complete six-jump cycle.

Assuming that each individual local energy barrier heights are proportional to the overall barrier height E_{gs}.

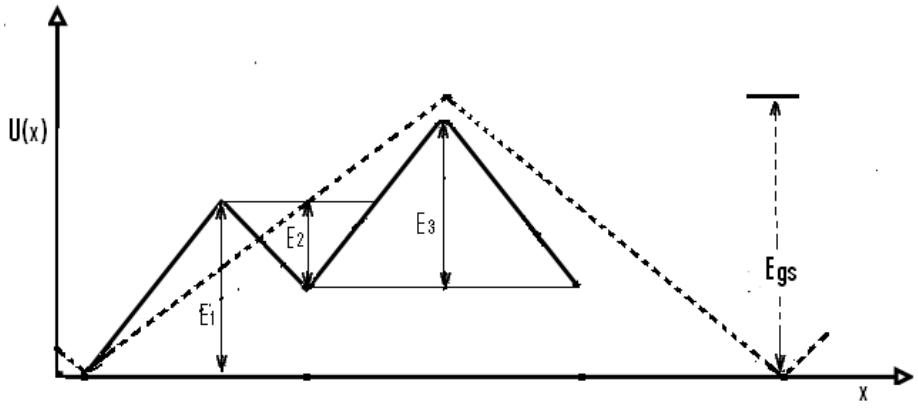

Figure 3.10: The relationship between the local energy barrier heights with the overall energy barrier height (broken lines) of six-jump mechanism.

$$E_1 = \alpha_1 E_{gs}; \qquad E_2 = \alpha_2 E_{gs} \tag{3.79}$$

and

$$E_3 = \alpha_3 E_{gs} \tag{3.80}$$

Where

- α_1, α_2,and α_3 is the proportionality constant between E_1, E_2, and E_3 with E_{gs}.

Substituting these values in Eq. 3.78, we will get

$$\alpha_1 - \alpha_2 + \alpha_3 = 1 \tag{3.81}$$

With this assumption, the MFPT expression of the six-jump cycle mechanism becomes as follows

$$\begin{aligned}\tau_s = \frac{4}{D_0}\exp[\beta E_{gs}] \Bigg[& 2\left(\frac{\Delta}{\beta(\alpha_1+\alpha_2)E_{gs}}\right)^2 \exp[\beta(\alpha_2-\alpha_3)E_{gs}] + \Bigg] \\ & + \left[2\left(\frac{\Delta}{\beta(\alpha_1+\alpha_2)E_{gs}}\right)^2 \exp[\beta(\alpha_2-\alpha_1)E_{gs}] + \left(\frac{\Delta}{\beta(\alpha_2+\alpha_3)}\right)^2 \exp[\beta(2\alpha_2-\alpha_3-\alpha_1)E_{gs}]\right] \\ & + \left[\left(\frac{\Delta}{\beta(\alpha_2+\alpha_3)E_{gs}}\right)^2\right]\end{aligned} \tag{3.82}$$

If we compare $exp[\beta E_{gs}]$ with the remaining terms of the equation such as $\exp[\beta(\alpha_2 - \alpha_3)E_{gs}]$ and $\exp[\beta(\alpha_2 - \alpha_1)E_{gs}]$ one can see that these terms are very very small.

Therefore, one can take the following approximations

$$\begin{aligned} \exp[\beta(\alpha_2 - \alpha_3)E_{gs}] &\simeq 0 \\ \exp[\beta(\alpha_2 - \alpha_1)E_{gs}] &\simeq 0 \\ \exp[\beta(2\alpha_2 + \alpha_3 - \alpha_1)E_{gs}] &\simeq 0 \end{aligned} \tag{3.83}$$

With this approximation and $\Delta = \Delta s$, lattice spacing of the six-jump mechanisms, the above equation reduces to

$$\tau_s \simeq \frac{4}{D_0}\left(\frac{\Delta s}{\beta(\alpha_2 + \alpha_3)E_{gs}}\right)^2 \exp[\beta E_{gs}] \tag{3.84}$$

Second, let us consider the triple defect mechanism where the vacancy completes its cycle within four lattice site as we have seen in the first chapter. In previous section, we derived as you see in Eq. 3.31, which is the MFPT of the vacancy diffusion in triple defect mechanism in terms of local jump probabilities. In the same fashion as of the six-jump mechanism, we can calculate MFPT of this mechanism in terms of local times and we have got the following MFPT expression of the vacancy in this mechanism in terms of local barrier heights. i.e,

$$\tau_t = \frac{4}{D_0}\exp[\beta E_{gt}]\left[2\left(\frac{\Delta}{\beta(\alpha_1+\alpha_2)E_{gt}}\right)^2\exp[\beta(\alpha_2-\alpha_3)E_{gtt}]+\right.$$
$$+\left[2\left(\frac{\Delta}{\beta(\alpha_1+\alpha_2)E_{gt}}\right)^2\exp[\beta(\alpha_2-\alpha_1)E_{gt}]+\left(\frac{\Delta}{\beta(\alpha_2+\alpha_3)}\right)^2\exp[\beta(2\alpha_2-\alpha_3-\alpha_1)E_{gt}]\right]$$
$$+\left.\left[\left(\frac{\Delta}{\beta(\alpha_2+\alpha_3)E_{gt}}\right)^2\right]\right. \tag{3.85}$$

If we compare $e^{[\beta E_{gt}]}$ with the remaining terms of the equation

$$\begin{aligned}\exp[\beta(\alpha_2-\alpha_3)E_{gt}] &\simeq 0 \\ \exp[\beta(\alpha_2-\alpha_1)E_{gt}] &\simeq 0 \\ \exp[\beta(2\alpha_2-\alpha_3-\alpha_1)E_g] &\simeq 0\end{aligned} \tag{3.86}$$

For $\Delta = \Delta t$, the above equation reduces to

$$\tau_t \simeq \frac{4}{D_0}\left(\frac{\Delta t}{\beta(\alpha_2+\alpha_3)E_{gt}}\right)^2\exp[\beta E_{gt}] \tag{3.87}$$

where

- E_{gt} is the overall energy barrier height within a one complete triple defect mechanism,
- α_2, α_3 is the proportionality constant between E_2 and E_3 with E_{gt}.

What we have seen from our result is that even though the MFPT of the vacancy in these two mechanisms is a function of local MFPTs (related to local energy barrier height) finally reduced to the overall energy barrier heights E_{gs} and E_{gt} respectively instead of these local barrier heights: E_1, E_2 and E_3.

The vacancy in next nearest neighbor (NNN) mechanism performs a jump of length, ΔN, from its own sublattice in a second neighbor lattice sites by crossing one local energy barrier height. Let us take this local energy and lattice space of the mechanism as its global one and compare with the other two previous mechanisms. Similarly using Eq. 3.38, which is the MFPT of the vacancy in NNN mechanism in terms of the local jump probability, one can obtain the MFPT of it in this mechanism in terms of local first passage time, which is equal to

$$\tau_N \simeq \frac{4}{D_0}\left(\frac{\Delta N}{\beta E_{g0}}\right)^2 \exp[\beta E_{g0}] \tag{3.88}$$

where

- $E_{g0} = E_0$ is the overall energy barrier height within a one complete NNN cycle,
- ΔN is the local as well as the periodic distance of NNN mechanism.

It is straight forward that the MFPT of the vacancy in NNN mechanism is a function of its global barrier height (E_0). Therefore, we can conclude that the MFPT taken by the vacancy to complete its different mechanisms is related to the overall energy barrier height which is identical result to [22].

Since the MFPT of these three mechanisms are a function of local and global energy barrier height, background temperature and lattice spacing. Now let us substitute the computed values of some these parameters to find the actual values of

vacancy's mean first passage time in these different mechanisms and compare these analytical result with the numerical ones that we have calculated in chapter three. Taking the background temperature at T = 1200k for all mechanisms but considering their own lattice space, local and global energy barrier heights, we calculated analytically the MFPT values of the vacancy along the different six-jump mechanisms and the other two mechanisms that is shown in Table. 3.1 and 3.2 respectively.

Table 3.1: The MFPT of the different six-jump mechanism at T = 1200k, the normal diffusion coefficient ($D_0 = 2.77 \times 10^{-6} m^2 s^{-1}$).
.

Mechanism	MFPT(s)	$E_1(ev)$	$E_2(ev)$	$E_3(ev)$	$E_{gs}(ev)$
Six[110]	2.2637×10^{-5}	2.34	0.33	0.56	2.58
Six[100]bent	7.9181×10^{-2}	2.87	0.68	1.41	3.60
Six[100]st	2.6945×10^{-1}	2.87	0.68	1.55	3.74

Table 3.2: The MFPT of the remanning two and one of the six-jump mechanisms at T = 1200k: global energy barrier heights(E_g), the normal diffusion coefficient (D_0) which is the experimental value [11].

Mechanism	MFPT(s)	$E_2(ev)$	$E_3(ev)$	$E_g(ev)$	$D_0(10^{-5} m^2.s^{-1})$
NNN	1.3767×10^{-6}	-	-	2.58	2.71
Six-jump[110]	2.2637×10^{-5}	0.33	0.56	2.58	2.77
Triple D	1.5387×10^{-12}	0.59	0.74	1.07	3.45

From Table 3.1, we can see that the MFPT taken by the vacancy to complete the six-jump mechanism through six[110] is smaller than the other two. From this analytical result, we can conclude that the vacancy favors this diffusion mechanism to diffuse through the NiAl compound than the others. The analytical MFPT values of the vacancy via the triple, NNN and six[110] (a representative of the collective six-jump mechanism) mechanisms is in Table 3.2. One can see that the MFPT of the vacancy in triple defect mechanism is smaller than the other two mechanisms. In

other words, this mechanism is the one which is favored by the vacancy to diffuse in NiAl compounds. Beside all of these, when we compare these individual analytical values with their simulation result that is computed by Adib's method in chapter two, we can observe that the computed MFPT value of the vacancy in NNN mechanism is, $< \tau_N >= 3.2762 \times 10^{-04}$, which is greater than its analytical one, 1.3767×10^{-6}. But for the two mechanisms, particularly for the triple one, the difference between the analytical and its simulation result is very small.

3.4 Calculation of the diffusion coefficient

In this section, we will calculate an effective diffusion coefficient of a vacancy when it diffuse via in those three vacancy diffusion mechanisms. As we have seen in the above section, the MFPT expressions of NNN, six-jump and triple defect mechanisms are related to the overall energy barrier heights. In the six-jump and triple defect mechanisms, we know that each local energy barrier heights are proportional to their global ones. First let us take the six-jump mechanism and its potential profile which can be represented by a figure like that is shown below, Fig. 3.11. From this graphical

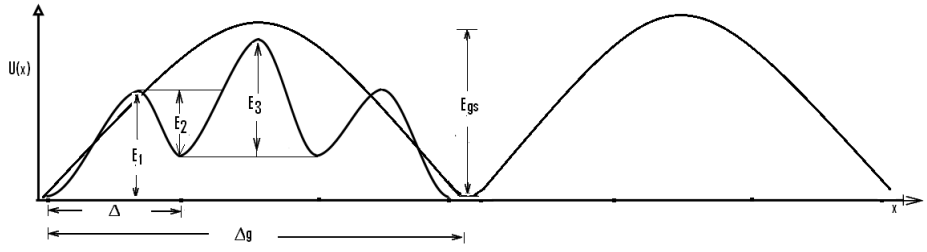

Figure 3.11: The relationship between the local barrier heights and lattice space with the global barrier height and lattice space of the six-jump mechanism

representation, we can get the maximum energy U_{max} which we call it global energy

barrier height just by taking the sum of local energy barrier heights.

$$U_{max} = E_{gs} = E_1 - E_2 + E_3 \tag{3.89}$$

where E_{gs} is the maximum or global energy barrier height that the vacancy crosses to complete the six-jump mechanism. If we assume vacancy diffusion in bulk NiAl, this single global process may repeats a number of times in addition to those local cycles. From now on, even though, the vacancy performs both its local cycles and global one, we are going to deal this global periodic motion by introducing the one-dimensional lattice of step size $3\Delta = \Delta g$ and the lattice sites are centered at the potential minima. The vacancy performs hops from one potential minimum to its neighbor sites by crossing this global potential. We can see that each global cycle repeat itself within a distance of Δ_g, or it is the potential period, $U(x) = U(x + \Delta_g)$. Therefore, one can model the vacancy motion in this periodic potential as a particle of mass m be under the influence of external total potential, U_{max}, in a one dimensional highly viscous medium of constant friction coefficient γ and temperature T where its dynamics can be governed by the Langevin equation. i.e

$$m\frac{d^2x}{dt^2} = -\gamma\frac{dx}{dt} - U^{'}(x) + \sqrt{2k_BT\gamma}\xi(t) \tag{3.90}$$

where

- x is the displacement in time t,
- T is the temperature,
- k_B is the Boltzmann constant and

- $\xi(t)$- is the Gaussian white noise

Note that $\xi(t)$, the white Gaussian noise with zero mean and correlation. i.e,

$$< \xi(t) >= 0 \tag{3.91}$$

and

$$< \xi(t) >< \xi(t^{'}) >= \sqrt{2k_BT\gamma}\sigma(t - t^{'}) \tag{3.92}$$

For viscous medium(very high friction medium) Eq. 3.90 can be simplified to

$$\frac{dx}{dt} = -\frac{U^{'}(x)}{\gamma} + \xi(t)\sqrt{\frac{2k_BT}{\gamma}} \tag{3.93}$$

In other words, this inertia term is assumed to have a negligibly small effect in comparison with the other forces appearing in the equation. For $dW(t) = \xi(t)(dt)$, one gets

$$dx = -\frac{U^{'}(x)}{\gamma}dt + \sqrt{\frac{2k_BT}{\gamma}}dW(t) \tag{3.94}$$

From this equation for the probability density $p(x, t \mid x_0, t_0) = p(x, t)$, we can get the corresponding Fokker-Planck equation(FPE)

$$\frac{\partial p(x,t)}{\partial t} = \frac{1}{\gamma}\frac{\partial \left[\beta U^{'}(x)p(x,t)\right]}{\partial x} + \frac{k_BT}{\gamma}\frac{\partial^2 p(x,t)}{\partial x^2} \tag{3.95}$$

where

- p(x,t) is the probability density of finding the particle at position x at time t given that it was initially at position x_0.
- $U^{'}(x) = \frac{U(x)}{dx}$ with U(x) being the potential function
- k_B the Boltzman constant and T is temperature

For large times, the drift is characterized by the mean stationary velocity.

$$\left\langle \frac{dx}{dt} \right\rangle = \lim_{t\to\infty} \frac{< x(t) >}{t} \tag{3.96}$$

The value of this quantity is zero. In our present study, the quantity of central interest will be the effective diffusion coefficient, which is given by

$$D = \lim_{t\to\infty} \frac{< x^2(t) > - < x(t) >^2}{2t} \tag{3.97}$$

where

- D is the effective diffusion coefficient

In simple words, the process described by Eq. 3.95 is physically equivalent to the motion of a particle in an infinite ordered set of segments of the effective potential U(x)= U_{max} as sketched in Fig. 3.12. Because of periodicity of the potential, i.e,

$$U(x + \Delta_g) = U(x) \tag{3.98}$$

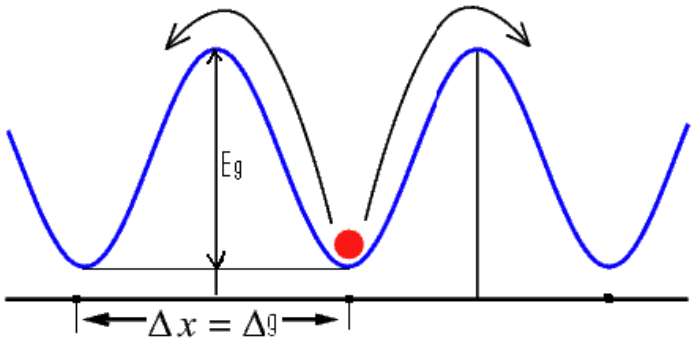

Figure 3.12: A vacancy hopping through its states by crossing the global barrier height E_g in the one dimensional lattice sites.

The diffusion process can be coarsely conceived as consecutive transitions of vacancy particle from points of potential minima $x_i = i\Delta_g$ to nearest neighboring points $x_{i\pm1}$. The transition time represents the escape time over left or right absorbing boundaries $x = x_{i\pm1}$ for a particle starting from the point $x = x_i$ i.e., the random mean first passage time. Thus, we can consider, as in reference [17], the discrete process or jumped diffusion model which is given by

$$x(t) = \sum_{i=0}^{n} \Delta_i \tag{3.99}$$

where

- Δ_i are random increments of jumps with values Δ_g and
- n denotes the total number of jumps in the time interval (0, t).

The random increments Δ_i and the random times τ_i between jumps are statistically independent of one another and have the same probability distributions of position

and time τ_i [5]. Because of the symmetry of the potential U(x), the probabilities of transitions to the left or right have the same value. Consider a one-dimensional random walk process with constant step size, Δ_i, and random time, τ_i, that is shown in Fig. 3.13. That means for a time, τ_n, the walker takes a step of length Δ_i to the

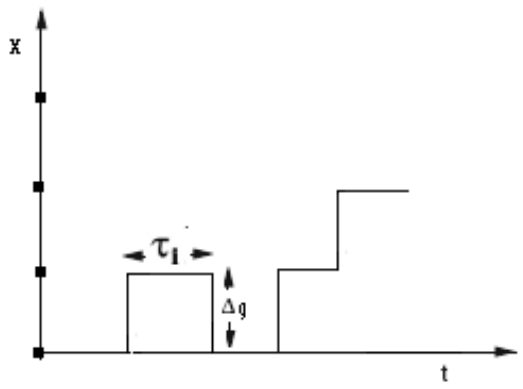

Figure 3.13: A vacancy sample trajectory where the random increments in position is $\pm\Delta_g$ and the intervals τ_i correspond to independent realizations of the mean first passage time.

left with probability q or right with probability p (p = q =1/2). The corresponding step size distribution function $P(\Delta_i)$ will be

$$P(\Delta_i) = \frac{1}{2}\left[\sigma(\Delta_i - \Delta_g) + \sigma(\Delta_i + \Delta_g)\right] \tag{3.100}$$

Let the walker start at $x(\tau_i) = 0$ then the probability $P_n(i)$ of reaching position $i\Delta x$ after n steps obeys the recursion

$$P_{n+1}(i) = \frac{1}{2}\left[P_n(i+1) + P_n(i-1)\right] \tag{3.101}$$

which obviously leads to a binomial distribution. From the expansion of this binomial distribution and since the steps are uncorrelated we easily find the first two moments [18]. First

$$< x(t) >= 0 \tag{3.102}$$

and second

$$< \Delta x^2(t) >= n\Delta_g^2 \tag{3.103}$$

On the other hand in the limit $t \to \infty$, we have that

$$n \simeq \frac{t}{\tau} \tag{3.104}$$

where $\tau =< \tau_j >$ is the MFPT of the vacancy as a particle with initial position x = 0 and absorbing boundaries at $x = \pm\Delta_g$. After substitution of Eq. 3.103, Eq. 3.104 in Eq. 3.97, we arrive finally at the exact result

$$D = \lim_{t\to\infty} \frac{< x^2(t) > - < x(t) >^2}{2t} = \frac{(\Delta_g)^2}{2\tau} \tag{3.105}$$

which was first derived in reference [19] for fixed periodic potential. As we have seen from potential profiles of thus different diffusion mechanisms, one global periodic

distance is equal to

$$\Delta_g = \begin{cases} \Delta N & \text{for NNN mechan} \\ 3\Delta s & \text{for six-jump mechan} \\ 3\Delta t & \text{for triple defect mechan} \end{cases} \tag{3.106}$$

In chapter two section 2.5, we have calculated numerically the MFPT of the vacancy in these mechanisms using Adib's algorithm and its three values are;

- $< \tau_N >= 3.2762 \times 10^{-04}$ sec for the NNN mechanism
- $< \tau_s >= 3.031554 \times 10^{-07}$ sec for the six-jump mechanism and
- $< \tau_t >= 5.509186 \times 10^{-12}$ sec for the triple defect mechanism.

Then the effective diffusion coefficients of the vacancy when it diffuse via the three diffusion mechanisms with these periodic distances and the above computed mean first passage time becomes as follows:

- $D_N = 1.2835 \times 10^{-16} m^2.s^{-1}$
- $D_s = 2.496 \times 10^{-12} m^2.s^{-1}$
- $D_t = 5.6723 \times 10^{-09} m^2.s^{-1}$

where D_N, D_s and D_t are the effective diffusion coefficient of NNN, six-jump, and triple defect mechanisms respectively. From these result, we can see that the diffusion coefficient of the triple defect is much larger than the other two.

Now let us substituting the MFPT expressions that we have derived in the previous section instead of their actual values from Adib's simulation algorithm. First let us see

the six-jump mechanism by substituting the mean first passage expression, Eq. 3.84 into Eq. 3.105 and we will get

$$D_s = \frac{D_0}{8}\left(\frac{\Delta_{gs}}{\Delta}\right)^2\left(\frac{(\alpha_2+\alpha_3)E_{gs}}{k_BT}\right)^2\exp\left(-\frac{E_{gs}}{k_BT}\right) \tag{3.107}$$

Since $\beta = \frac{1}{k_BT}$, this is the effective diffusion coefficient of the six-jump mechanism. From Fig. 3.11, we can see that within one six-jump cycle we have three local lattice spacing, Δ. That is, $\Delta_g = 3\Delta$, because of this the above diffusion equation simplify to

$$D_s = \frac{9D_0}{8}\left(\frac{(\alpha_2+\alpha_3)E_{gs}}{k_BT}\right)^2\exp\left(-\frac{E_{gs}}{k_BT}\right) \tag{3.108}$$

Similarly, the diffusion coefficient of the triple defect mechanism with the substitution of the corresponding periodic distance and MFPT is given by

$$D_t = \frac{9D_0}{8}\left(\frac{(\alpha_2+\alpha_3)E_{gt}}{k_BT}\right)^2\exp\left(-\frac{E_{gt}}{k_BT}\right) \tag{3.109}$$

and finally, the diffusion coefficient of the NNN mechanism is

$$D_N = \frac{D_0}{8}\left(\frac{E_{g0}}{k_BT}\right)^2\exp\left(-\frac{E_{g0}}{k_BT}\right) \tag{3.110}$$

Except for the pre-exponential factors, the effective diffusion coefficients of the three mechanisms are similar to the one in chapter one in Eq 1.1 which obeys the Arrhenius

law. The overall energy(Q) in that equation is identical to the global energy barrier height (E_g). The effective diffusion coefficient of all mechanisms are a function global energy barrier height and in particular, the six-jump and the triple defect mechanisms are a function of the local barrier heights beside the global one. Moreover, the six-jump mechanism that we saw in chapter one has three different paths of a vacancy to complete its cycle. These three different six-jump mechanisms are: Six[110], Six[100]straight and Six[100]bent. using computed values of the local as well as the global energy barrier heights and the experimental normal diffusion coefficients, we tried to calculate the effective diffusion coefficients of these mechanisms and their values are shown in table 3.3, note D denotes the effective diffusion coefficient. From this

Table 3.3: The effective diffusion coefficient(D) values of the three different six-jump mechanisms at T = 1200k: global energy barrier heights(E_g), local energy barrier heights(E_2, E_3), and the free diffusion coefficient(D_0) which is the experimental value calculated by [11].

Mechanism	$D(m^2.s^{-1})$	$E_{gs}(ev)$	$E_2(ev)$	$E_3(ev)$	$D_0(10^{-5}m^2.s^{-1})$
Six[110]	3.3433×10^{-14}	2.58	0.33	0.56	2.77
Six[100]st	2.8718×10^{-18}	3.74	0.68	1.55	2.77
Six[100]bent	9.556×10^{-18}	3.60	0.68	1.41	2.77

analytical result we can see that the effective diffusion coefficient of the [110]Six-jump is larger than the two remaining six-jump mechanisms. The effective diffusion coefficients of the other two remaining mechanisms is in table 3.4. In general, what we have seen from these tables, the effective diffusion coefficient of the triple defect is larger than the two remaining mechanisms. If we get the experimental diffusion coefficient value of the three mechanisms, we can evaluate our analytical result and also validate our methodology. In all three cases, the effective diffusion coefficient(D) of vacancy are a function of the background temperature(T), local barrier heights and as well as

Table 3.4: The effective diffusion coefficient(D) values of the two remaining mechanisms at T = 1200k: note that the values of these parameters are computed by [11].

Mechanism	$D(m^2.s^{-1})$	$E_{g0}/E_{gt}(ev)$	$E_2(ev)$	$E_3(ev)$	$D_0(10^{-5}m^2.s^{-1})$
NNN	3.054×10^{-14}	2.58	–	–	2.71
Triple D	2.053×10^{-7}	1.07	0.59	0.74	3.45

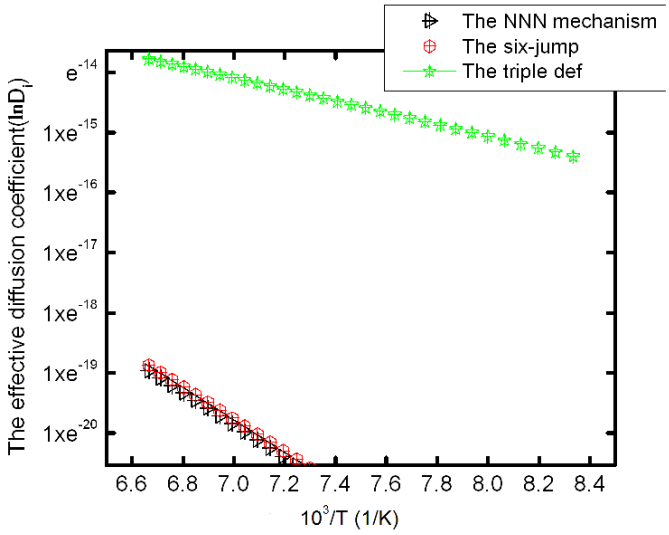

Figure 3.14: The effective diffusion coefficients of the three mechanisms as a function of temperature.

global barrier heights. To see the effect of temperature on the effective diffusion coefficients(D) of the three mechanisms, we have taken the overall energy heights of each mechanism. See table 3.3 and 3.4 for the local, global energy barrier heights and the free diffusion coefficient values of these mechanisms. With these values we vary the temperature from 1200k to 1500k to see its effects on diffusion coefficient. Fig 3.14 compares the effective diffusion coefficients (D) of the three mechanisms between that temperature interval. As clearly seen see from this figure, the value of D increases as the background temperature increases. At all temperature levels, the triple defect

mechanism has the highest value of all and the two have nearly the same value at high temperature. Therefore, we can conclude that the triple defect is the main route for vacancy diffusion at any temperature and the six[110] and the NNN mechanisms may contribute for vacancy diffusion when temperature is high. Furthermore, our result of the temperature dependence of effective diffusion of a vacancy in NiAl by these mechanisms was found to obey the Arrhenius law (see chapter one).

Chapter 4

Summary and conclusion

In the present thesis, we have carried out a compressive investigation of vacancy's Mean First Passage Time (MFPT) and effective diffusion coefficient (D) when it diffuse via the three main vacancy diffusion mechanisms of NiAl binary alloy both numerically and analytically. We used first passage algorithm of R. Adib [1] and the Goldhirsch and Gefen [8] technique to solve these vacancy problem numerically and analytical respectively.

These three vacancy diffusion mechanisms are: the next nearest neighbor (NNN), six-jump, and the triple defect mechanism. In Next-nearest-neighbor mechanism, a vacancy (which may be due to a missing atom of either of the two) jumps a distance of ΔN to next nearest-neighbor of its kind by crossing the corresponding energy barrier height. In the six-jump mechanism a vacancy takes three successive cyclic displacements of each a distance Δs between the two sublattices. This mechanism in principle can occur by three different pathways, one of which results in a vacancy moving in the [110] direction whereas the other two paths move a vacancy in the [100] direction. The triple defect mechanism, consists of four NN jumps of distance Δt initiated by a two vacancies and antisite atom which is created somewhere in the two sublattices of NiAl. Note that for the last two mechanisms, when the vacancy

jumps from one lattice site to the next site, it crosses an energy barrier height which are related to each meta stable or stable states.

The above three diffusion mechanisms of the vacancy over the NiAl crystal structure is modeled by a one dimensional walk of the vacancy over one dimensional lattice sites ($x_i = i\Delta_i$) with a lattice distance Δ_i. In this one-dimensional system, a vacancy jumps at each point of time from its current position x_i to the position $x_i \pm \Delta_i$ with some transition rates (jump probability per unit time) where these local rates may depend on the location along the lattice sites. For our model, the local transition rates along the path of the different diffusion mechanisms have been calculated from their local potential profiles, $U(x_i)$ using [1] method. i.e, $k(x_i \pm \Delta \mid x_i) = \frac{D_0}{(\Delta)^2} \exp\left(\mp \frac{U^{'}(x)\Delta}{2k_BT}\right)$. As you might see from this expression, transition rates are a function of lattice space (Δ_i), local energy barrier height ($U^{'}(x)\Delta$), free diffusion coefficient (D_0), and temperature (T). Since vacancy diffusion is due to thermal energy, we compared the transition rates of the three different six-jump mechanisms within themselves and with the other two mechanisms by varying the background temperature from 1200 to 1500k. We have used Table. 2.1 for values of the above controlling parameters of the six-jump mechanisms and we vary the temperature in that specified range and we have found that all of them increase with temperature that is shown in chapter two of Fig. 2.9(a). When we compared them, we found that [100] straight six-jump rate has the lowest of all whereas [110] six-jump has the highest at all temperature. But at high temperature, six[100] bent has nearly the same value of that of six[110]. Then, we can conclude that [110] six-jump is a favorable path for vacancy diffusion at all temperature but six[100] bent may contribute for diffusion at high temperature in NiAl among these different six-jump mechanism.

On the same fashion, taking the overall energy barrier heights and other controlling parameters from Table. 2.2 for the NNN, triple defect and the six[110] jump (which represent the collective six-jump) diffusion mechanisms compared their rates in the above temperature intervals and it is shown in Fig. 2.9(b). The figure clearly shows that all of them increase with temperature and the triple defect mechanism has the highest rate of all mechanisms at all temperature. At higher temperature all of them may contribute for vacancy diffusion. In general, NNN and six-jump mechanisms are unfavorable vacancy diffusion paths where as the triple defect is the most favorable path for vacancy diffusion in NiAl even at low temperature. In addition, both figures show that our result of transition rate versus temperature obeys the Arrhenius laws.

The time evolution of the vacancy on this one-dimensional lattice system is governed by a master equations where numerically this equation could be solved by Adib simulation algorithm [1]. According to this algorithm, one places a vacancy in one of its meta or stable states x_i and then determine the lifetime of the vacancy in that state from an exponentially distributed random number τ_i with mean equal to the reciprocal of the sum of the outgoing rates, i.e $< \tau_i >^{-1} = \sum_{x_i'=n.n} k(x_i' \mid x_i)$ and the nearest neighbor state where the vacancy next jumping position is chosen with a weighting factor, $w(x_i) = \frac{k(x_i'|x_i)}{\sum_{x_i'=n.n} k(x_i'|x_i)}$ among the possible neighbor sites. The vacancy then moves to this chosen state, and the procedure above is repeated until it touches an absorbing state of each mechanism. The sum of the times $< \tau_i >$ until this criterion is satisfied is then the first passage time of that mechanism. During each step, we trace the position as well as the time of the vacancy until it touches its absorbing site. Figs. 2.11(a), 2.11(b) and 2.11(c) are position versus first passage time of the vacancy for NNN, six-jump and triple defect mechanisms. Their trajectories

show a discrete space and continuous time which is identical to the one calculated by Adib [1].

Mean while, from this simulation algorithm, we have calculated the mean first passage times and effective diffusion coefficients of of the vacancy when it diffuse via these above mechanisms and their values are given as follows:

- NNN mechanism, $< \tau_N >= 3.2762 \times 10^{-04}$ sec, $D_N = 1.2835 \times 10^{-16} m^2.s^{-1}$
- For Six-jump, $< \tau_s >= 3.0316 \times 10^{-07}$ sec, $D_s = 2.946 \times 10^{-12} m^2.s^{-1}$
- Triple defect, $< \tau_t >= 2.0406 \times 10^{-11}$ sec, $D_t = 1.908 \times 10^{-08} m^2.s^{-1}$

This simulation result shows that the triple defect mechanism takes shorter time and has the larger effective diffusion coefficient than the other two. From this result we concluded that the vacancy diffuse more easily via triple defect than the other two mechanisms in NiAl binary alloys.

In that one-dimensional lattice sites system, a vacancy at site x_i hops to its nearest neighbor sites with a local probability (p or q) instead of the local transition rates k_i that we have used previously. Simply we place the vacancy in any state of the system and allow it to jump either to the left with its local probability q or to the right with local probability p. After specifying the absorbing edges of the lattice sites of our system, we derived the mean first passage time expression of the vacancy analytically using Goldhirsch and Gefen [8] technique. These MFPT expressions of the vacancy to complete each above three mechanisms are a function of vacancy‘s local jump probabilities, p_i and q_i that is given in Eq. 3.75, Eq. 3.31, Eq. 3.38 for the three of them.

According to Kramer rule, these local jump probabilities, p_i or q_i is the inverse

of the local mean first passage time, τ_i, which we calculated it from the piece-wise linear potential profile that the vacancy crosses [6] along its different paths. This local mean first passage times are a function of local energy barrier height(E_i), the background temperature of the system(k_BT), and the lattice spacing, Δ_i. Finally we substitute local mean first passage times instead of local jump probabilities, p_i or q_i in those MFPT expressions and we have found that the MFPT taken by the vacancy to complete its different mechanisms is a function of local as well as the global energy barrier heights, temperature and lattice space which is in agrement with [22]. These MFPTs are given in Eq. 3.84, Eq. 3.87, Eq. 3.88 for the three different mechanisms. Using experimental values of the free diffusion coefficient, D_0, computed values of local as well as global energy barrier heights, the MFPT expressions of each individual mechanisms are evaluated and their analytical values are shown below;

- Six-jump, $< \tau_s >= 8.4112 \times 10^{-6} s$
- Triple D, $< \tau_t >= 1.370 \times 10^{-12} s$
- NNN Mech, $< \tau_N >= 1.3767 \times 10^{-6} s$

In this analytical result shows that the vacancy takes less time when it diffuse via the triple defect mechanism than the other two mechanisms. It also indicates that the vacancy favorers the triple defect mechanism for its diffusion process in NiAl. In addition, this analytical result of six-jump and triple defect mechanisms is nearly in agrement with the numerical result, calculated by Adib's method, in chapter two section 2.5.

From the potential profiles of the six and triple defect mechanisms, one can see that there are three local energies at the three different sites of these mechanisms.

This kind of potential structure lead us to postulate another model of vacancy walk in one-dimensional lattice of length, $\Delta g = 3\Delta_i$, by crossing a maximum energy $U(x) = E_1 - E_2 + E_3$ which we call it global energy barrier height. This will address the problem of the vacancy executing a random walk in a spatially varying periodic potential $U(x) = U(x + \Delta g)$ with period Δg. The lattice step size Δg is equal to the potential period and the lattice sites are centered at the potential minima. Using this same analytical technique, the problem of the effective diffusion of the vacancy in those global symmetric periodic potentials were calculated and its result reduced to the mean first passage time and the global lattice space. Since the MFPT of each mechanism is function of local as well as the global energy barrier heights, temperature and lattice space, to solve analytically, we substituted computed values of these parameters and we have got the following values of effective diffusion coefficient of the vacancy for the three different six-jump mechanisms;

- Six[100]st, $2.8718 \times 10^{-18} m^2.s^{-1}$
- Six[100]bent, $9.556 \times 10^{-18} m^2.s^{-1}$
- Six[110], $3.3433 \times 10^{-14} m^2.s^{-1}$

The vacancy's D for the two remaining mechanisms have the following analytical values;

- Triple D, $2.053 \times 10^{-7} m^2.s^{-1}$ and
- NNN , $3.054 \times 10^{-14} m^2.s^{-1}$

In comparison, these results indicates that the effective diffusion coefficient of the vacancy via [110]Six-jump is larger than the two remaining six-jump mechanisms.

Including the [110]Six-jump, we compared the NNN and triple defect mechanisms effective diffusion coefficient of the vacancy and we have found that the vacancy D in triple defect is greater than the NNN and the [110]Six-jump mechanisms. The effective diffusion coefficients of the vacancy in the three mechanisms is analyzed as a function of temperature and it is shown in Fig 3.14 where all value of D increases as the background temperature increases. Therefore, our result of the temperature dependence of effective diffusion of a vacancy in NiAl by these mechanisms was found to obey the Arrhenius law, see chapter one.

As a whole, we have found that the vacancy when it diffuse via [110]six-jump and triple defect mechanisms has the highest rate and diffusion coefficient and it has taken lowest time to complete its diffusion mechanisms among their groups. This is mainly due to the fact that the vacancy crosses small local and overall energy barrier heights when it diffuse via these two mechanisms compared with the others. Our result is in consistent with Marino and Carter [11] result where they used first-principles density functional theory to calculate Ni diffusion in NiAl and their findings indicated that both the triple defect mechanism and [110] six-jump mechanism are likely contributors to this diffusion process. An additional verification is essential since we have been used Adibs's algorithm for a vacancy MFPT calculations which is based on one or two sublattice and these sublattices are very small compared with the size of bulk intermetallic compound NiAl.

To sum up, this work can be extended to study the MFPT of a vacancy in three dimensional ordered binary alloys as most alloys in nature exist in three dimensions. Finally, the problem that we solved can also be resolved by using other computer simulation techniques, and we hope that experiments can be done to check these

mechanisms and their result we present in this thesis. As a concluding remark, we would like the need to relate our findings and methodology to experimental results.

Bibliography

[1] Artur B. Adib. *Phys. Rev. E.*, 80, 2009.

[2] M. P. Allen and D. J. Tildesley. *Computer Simulation of Liquids.* Clarendon Press, Oxford, 1987.

[3] R. Drautz and M. Fhnle. *Acta Metallurgica et Materiala.*, 47, 1999.

[4] E. W. Elcock and C. W. McCombie. *Phys. Rev.*, 109, 1958.

[5] Y. Galperin and J. Feder. *Statistical Physics.* Academic Press, New York, 1980.

[6] C. W. Gardiner. *Hand book of stochastic methods for physics, chemistry and natural sciences.* Springer-Verlag, 1990.

[7] Daniel T. Gillespie. A general method for numerically simulating the stochastic time evolution of coupled chemical reactions. *J. Comp. Phys*, 22:403–34, 1976.

[8] I. Goldhirch and Y. Gefen. *Phys. Rev. A*, 33, 1986.

[9] G. Van Kampen. *Stochastic processes in physics and chemistry.* NHPL, 1992.

[10] M. Koiwa M. Arita and S. Ishioka. *Acta Metall.*, 37, 1989.

[11] Kristen A. Marino and Emily A. Carter. *Physical Review B*, 78, 2008.

[12] D. B. Miracle. *Mater. Res. Symp*, 4, 1993.

[13] D. B. Miracle. *Acta Metall. Mater.*, 41, 1993.

[14] Y. Mishin and D. Farkas. *Philos. Mag. A*, 75, 1997.

[15] M. van Gend N. A. Stolwijk and H. Bakker. *Philos. Mag. A*, 42, 1980.

[16] Lee C M Neumann. J. P, Chang. Y. A. *Acta Metall*, 24, 1976.

[17] H. Linde P. Reimann, C. Van den Broeck. *Phys. Rev. Lett.*, 87:010602, 2001.

[18] Philipp O. J. Scherer. *Simulation of Classical and Quantum Systems*. Springer, Berlin Heidelberg, 2010.

[19] D. L. Weaver. *Physica A.*, 98:359, 1979.

[20] J. H. Westbrook and R. L Fleischer. *Basic mechanical properties and lattice defects of intermetallic compounds*. John Wily Sc Sons, LTD, New york, 2000.

[21] A. Y. Lozovoi Y. Mishin and A. Alavi. *Phys. Rev. B.*, 67, 2003.

[22] M. Asfaw Z. Getahun and M. Bekele. Competing jump cycles for vacancy diffusion in binary alloys. *Cond matt*, 2, 2008.

Appendix A

Poisson distribution

The Poisson distribution is particularly important for this thesis, since it characterizes process like the birth-and-death, production and decay of a chemical reaction, $\cdots$ and also plays a crucial role in the implementation of Gillespies algorithm.

Consider the following situation. You are waiting for a bus on a street corner and have been told that these pass by in a 'completely random' fashion. More precisely, in a small time interval of duration Δt, the chance that a bus arrives is approximately proportional to Δt, and does not depend upon the previous history. Let N denote the number of buses passing during the interval[0,t] . Suppose there is a positive constant λ the arrival rate, such that for any small time interval(t,t+Δt], the probability of a single arrival is approximately $\lambda\Delta t$ and the probability of no arrival is approximately $1 - \lambda\Delta t$. These probabilities are assumed to be independent of occurrences in [0,t]. Specifically,

$$P\left[N(t + \Delta t) = n + 1 \mid N(t) = n\right] = \lambda\Delta t + o(\Delta t) \tag{A.1}$$

and

$$P\left[N(t+\Delta t)=n \mid N(t)=n\right]=1-\lambda\Delta t+o(\Delta t) \tag{A.2}$$

Note that the two conditions ensure that

$$P\left[N(t+\Delta t)>n+1 \mid N(t)=n\right]=o(\Delta t) \tag{A.3}$$

Such a process is a Poisson process. It has the following important properties:

1. Independent increments. The numbers arriving in non overlapping intervals are independently distributed. This is the Markov or 'loss of memory' property.
2. The chance of two or more arrivals in a small time interval may be neglected.
3. Stationary increments. The distribution of the number of arrivals in an interval depends only on the duration of the interval.

The probability distribution of N can be derived as follows. Define $p_n(t) = P(N(t) = n)$. Conditioning on the number of arrivals in [0,t], gives us

$$p_n(t+\Delta t)=P_{n-1}(t)\left[\lambda\Delta t+o(\Delta t)+\right]+P_n(t)\left[1-\lambda\Delta t+o(\Delta t)+\right]+o(\Delta t) \tag{A.4}$$

Note that the first term on the right-hand side of Eq A.4 is the probability that there are $n-1$ arrivals in [0, t] and one arrival in $(t+\Delta t]$. The second term is the

probability that there are n arrivals in [0,t] and no arrivals in $(t + \Delta t]$. There is no need to consider any other possibilities as the Poisson axioms allow the occurrence of two or more arrivals to be neglected in a small time interval. Eq A.4 is valid for $n \geq 1$ and also for n = 0. If the convention is adopted that $P_{-1}(t) = 0 \quad \forall x \in \mathbf{t}$. Now rewrite as

$$\frac{p_n(t + \Delta t) - p_n(t)}{\Delta t} = \lambda p_{n-1}(t) + \lambda p_n(t) + \frac{o(\Delta t)}{\Delta t} \tag{A.5}$$

and take the limit as $\Delta t \to 0$. Then

$$p_n^{'}(t) = \lambda p_{n-1}(t) + \lambda p_n(t) \tag{A.6}$$

To solve this, multiply through by $e^{\lambda t}$ and rewrite as

$$\frac{d}{dt}\left[e^{\lambda t} P_n(t)\right] = \lambda \left[e^{\lambda t} P_{n-}(t)\right] \tag{A.7}$$

Solving this for n, it gives

$$P_n(t) = \frac{e^{-\lambda t}(\lambda t)^n}{n!} \tag{A.8}$$

which is a Poisson distribution with mean and variance both equal to λt.

A.1 Numerical implementation of a Poisson process.

For both homogeneous and inhomogeneous Poisson processes, and for a choice of time step Δt such that $r\Delta t < 1$, one draws at each time step a uniformly distributed random number x_{rand} between 0 and 1. If $r\Delta t > x_{rand}$ an event takes place. This method is based on the fact that for sufficiently small Δt, $P(1) = r\Delta t$, and $P(0) = 1 - r\Delta t$.

A.2 Time distribution between successive events for a constant rate Poisson process.

Suppose an event occurred at time t. What is the probability $P(\tau)$ that the next one takes place between $t + \tau$ and $t + \tau + d\tau$? One can decompose the probability in the following way:

$$P(\tau) = \text{(probability that no event takes place between t and t + } \tau \text{)} \times \text{(probability that one event occurs between } t + \tau \text{ and t + } \tau + d\tau \text{)} \quad \text{(A.9)}$$

or formally

$$P(\tau) = e^{(-\lambda\tau)\times\lambda d\tau} \quad \text{(A.10)}$$

where

- λ is the constant rate of the Poisson process.

The probability density function for successive time intervals is therefore a decaying exponential

$$P(\tau) = \lambda e^{(-\lambda\tau)} \tag{A.11}$$

With mean

$$< \tau >= \frac{1}{\lambda} \tag{A.12}$$

and the variance

$$< \tau^2 >= \frac{2}{\lambda^2} \tag{A.13}$$

A.3 Random numbers from non-uniform distributions.

Good random numbers play a central part in Monte Carlo simulations. Usually these are generated using a deterministic algorithm, which produces a sequence of numbers which have sufficiently random-like properties (despite being fully deterministic). The numbers generated this way are called pseudo-random numbers.

The pseudo random generators return a random number from uniform distribution U[0, 1) or U(0, 1) or some other combination of the limits. However, usually we need random numbers from non-uniform distribution. We shall now discuss how the raw material from the generators can be transformed into desired distributions. Even though there are a lot of methods which transform a random number from uniform to other form of a distribution. Let us take exact inversion method among these.

A.3.1 Exact inversion.

In general, probability distributions are functions, which satisfy

$$\int dx p(x) = 1, \qquad p(x) \geq 0, \text{for all x} \tag{A.14}$$

Here the integral goes over the whole domain where p(x) is defined. The fundamental transformation law of probabilities is as follows: if we have a random variable x from a (known) distribution, $p_1(x)$, and a function y = y(x), the probability distribution of y, $p_2(y)$, is determined through

$$p_1(x)|dx| = p_2(y)|dy| \tag{A.15}$$

or

$$p_2(y) = p_1(x)\frac{|dx|}{|dy|} \tag{A.16}$$

Now we know the distribution, $p_1(x)$, and we also know the desired distribution $p_2(y)$, but we do not know the transformation law y = y(x). It can be solved by integrating the above differential equation:

$$\int_{a_1}^{x} dx^{'} p_1(x^{'}) = \int_{a_2}^{y} dy^{'} p_2(y^{'}) \tag{A.17}$$

which is equal to

$$P_1(x) = P_2(y), \quad \text{or} \quad y = P_2^{-1}[P_1(x)] \tag{A.18}$$

where $P_1(x)$ is the cumulant of the distribution $p_1(x)$. a_1 and a_2 are the smallest values. Now $p_1(x) = 1$ and $x\epsilon[0,1]$. Thus, $P_1(x) = x$, and y is to be inverted from the equation

$$x = \int_{a_2}^{y} dy^{'} p(y^{'}) \tag{A.19}$$

This is the fundamental equation for transforming random numbers from the uniform distribution to a new distribution p(y). Unfortunately, often the integral above is not very feasible to calculate, not to say anything about the final inversion (analytically or numerically).

A.3.2 Exponential distribution.

Normalized exponential distribution for y $\epsilon[0,\infty)$ is $p(y) = e^{-y}$. Thus, now the transformation is

$$x = \int_{0}^{y} dy^{'} e^{-y^{'}} = 1 - e^{-y} \tag{A.20}$$

which will be

$$y = -ln(1-x) = -ln(x) \tag{A.21}$$

We can use x or $1 - x$ above because of the uniform distribution; one should choose

the one which does not ever try to evaluate ln 0.